©2014 Society of Economic Geologists, Inc.
Economic Geology, v. 109, pp. 1117–1135

Marine Volcanosedimentary Basins Hosting Porphyry Au-Cu Deposits, Cadia Valley, New South Wales, Australia*

Anthony C. Harris,[1,†] Ian G. Percival,[2] David R. Cooke,[1] Richard M. Tosdal,[3] Nathan Fox,[1] Charlotte M. Allen,[4] Ian Tedder,[5] Colin McMillan,[5] Paul Dunham,[5] and Dean Collett[5]

[1] *CODES ARC Centre of Excellence in Ore Deposits, University of Tasmania, Private Bag 126, Hobart, Tasmania 7001, Australia*

[2] *Geological Survey of New South Wales, Department of Primary Industries, Londonderry, New South Wales 2753, Australia*

[3] *Mineral Deposit Research Unit, University of British Columbia, Vancouver, British Columbia V6T 1Z4, Canada*

[4] *Research School of Earth Science, Australian National University, Australian Capital Territory 0200, Australia*

[5] *Newcrest Mining Limited, 600 St. Kilda Road, Melbourne 3004, Australia*

Abstract

The volcanosedimentary rocks that host the Au-rich porphyry Cu deposits of the Cadia Valley preserve the products of episodic volcanism that erupted into a large sedimentary basin. Volcanogenic sedimentation, including the Forest Reefs Volcanics, overwhelmed the fine-grained sedimentary component that characterized much of the Weemalla Formation. The Forest Reefs Volcanics evolved as a relatively low relief, multiple-vent submarine volcanic complex. The vents comprised mafic to intermediate lava flows, cryptodomes, and subvolcanic intrusions (dikes and sills). Stacked lava sequences, including hyaloclastites, massive lavas, and their reworked equivalents, are up to 1 km thick, forming significant intrabasinal topography. Explosive volcanism occurred during the late stages of Forest Reefs Volcanics deposition. These air-fall deposits, combined with coexisting shallow-water faunal assemblages, imply that volcanism became locally emergent. Continuity of sedimentation between underlying deep marine basin deposits of the Weemalla Formation and Forest Reefs Volcanics, coupled with the predominance of sheet-like, laterally continuous debris flow and other coarse-grained sedimentary deposits, implies that volcanism and related sedimentation persisted in an active sedimentary basin marginal to an oceanic island arc.

Deposition of the Forest Reefs Volcanics spanned the Late Ordovician to Early Silurian. Monzonite fragments (identical to the ore-related intrusions) are abundant in sedimentary breccias found at the top of the preserved volcanic stratigraphy. This finding, combined with available absolute ages of crosscutting intrusions and associated hydrothermal alteration and mineralization, suggests that some volcanosedimentary units were deposited synchronously with or immediately after the last known porphyry-related hydrothermal event in the Cadia Valley. The Au-rich porphyry deposits were therefore emplaced into an evolving sedimentary basin with episodic intrabasinal magmatism. Permeable horizons and volcanic lithofacies can preferentially host alteration and mineralization that can extend over several kilometers in lateral extent. This finding suggests that hydrological models of fluid flow in porphyry systems need to take basin architecture into account.

Introduction

Porphyry Cu-Au-Mo deposits form at shallow crustal levels, typically at depths of 1 to 3 km below the Earth's surface. As such, the landforms that occur above porphyry ore deposits are typically eroded, and it can be difficult to resolve them accurately in ancient systems. Although common perception is that porphyry ore formation occurs beneath stratovolcanoes, detailed volcanic facies analysis and geochronology in major porphyry belts suggest that a stratovolcanic setting is unlikely. Rather, porphyry ore deposit formation occurs in a variety of contrasting environments, including volcanosedimentary basins (Harris et al., 2006; Cooke et al., 2007). Such an environment can act to localize porphyry deposits but, more importantly, also has the potential to bury them to ensure subsequent preservation through geologic time.

The Cadia Valley, central New South Wales, hosts some of the oldest and largest known Au-rich porphyry Cu deposits (Fig. 1; Holliday et al., 2002; Wilson et al., 2003). Late Ordovician to earliest Silurian magmatism is associated with the emplacement of over 52 million ounces of gold (see mineral resources and ore reserves statements, www.newcrest.com.au). The combined metal endowment from five porphyry-related deposits makes Cadia Valley Australia's premier porphyry ore district. Volcanosedimentary rocks of the Forest Reefs Volcanics host the Au-rich Ridgeway and the giant Au-Cu Cadia East deposits. Geologic studies of the Cadia district have focused on the nature of the Au and Cu alkalic porphyry deposits and associated skarn mineralization (e.g., Harper, 2000; Holliday et al., 2002; Wilson, 2003; Wilson et al., 2003, 2007a, b; Forster et al., 2004; Kitto, 2005). Published and unpublished descriptions of the volcanosedimentary rocks of the Forest Reefs Volcanics have focused around the mineralized centers (Holliday et al., 2002; Wilson, 2003; Kitto, 2005), with limited regional correlation (Squire, 2001; Squire and McPhie, 2007). There have been extensive geochronological and geochemical analyses of the intrusive rocks associated with mineralization (Blevin, 2002; Wilson, 2003; Wilson et al., 2007a), but the age of the regional volcanosedimentary host rocks is still poorly constrained.

† Corresponding author: e-mail, Anthony.Harris@newcrest.com.au

*A digital supplement to this paper is available at http://economicgeology.org/ and at http://econgeol.geoscienceworld.org/.

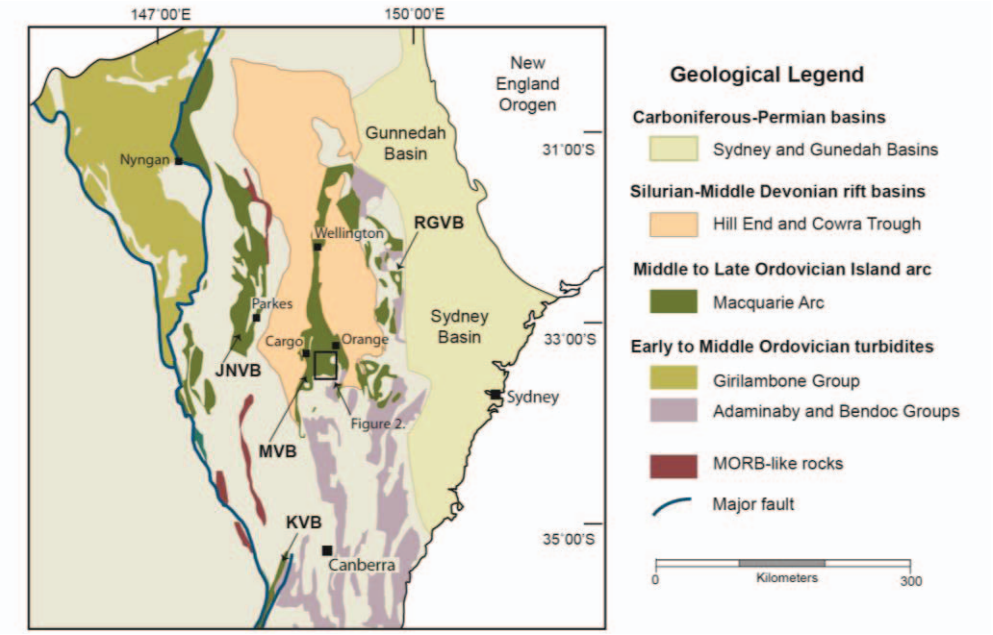

FIG. 1. Geology of the Late Ordovician Macquarie Arc of New South Wales. The Ordovician Molong volcanic belt (MVB) is one of the four segments of the dismembered oceanic arc. These volcanic belts formed together as part of one arc and were disrupted during rifting of the Hill End and Cowra trough. Middle to Late Ordovician rocks of the Junee-Narromine volcanic belt (JNVB) preserve the center of the volcanic arc, where basaltic andesitic and andesitic stratovolcanoes are the expression of suprasubduction zone magmatism (e.g., Simpson et al., 2007). The Molong volcanic belt comprises multiple packages of volcanic and volcaniclastic rocks, including the Forest Reefs Volcanics, host to the Cadia Valley porphyry Au-Cu deposits. The arc-related andesitic succession is dominated by thick sequences of volcanosedimentary breccias with volumetrically minor lavas (Squire, 2001). The volcaniclastic rocks conformably overlie and interfinger with fine-grained turbidites deposited in a restricted sedimentary basin east-southeast of an arc-like volcanic succession. A thicker apron of deep marine turbidites and fine-grained volcaniclastic rocks filled a more extensive basin that developed to the east of the Cadia district, occurring as the arc volcanic rocks of the Rockley-Gulgong volcanic belt (RGVB). KVB = Kiandra volcanic belt.

Our study provides new geologic descriptions of volcanosedimentary units from across the Cadia district. Reconstruction of the facies architecture of the volcanic sequences that host these deposits is used to help interpret the environment of formation and, more importantly, the environment that ensured their preservation. Measured stratigraphic sections and detailed documentation of the facies architecture help in the reconstruction of this ancient porphyry ore district. We use the distribution of volcanic, sedimentary, and hypabyssal lithofacies to infer the evolution of the arc-related marine basin and discuss its significance for porphyry Au-Cu mineralization and also for the tectonomagmatic evolution of the district.

Methods

The juxtaposition and intercalation of coherent and clastic lithofacies in the Cadia district make the recognition of laterally extensive stratigraphic markers difficult. Despite this, compositional similarities may exist between lavas and closely associated clastic (that includes both freshly eruptive and reworked) material. Assuming compositional similarities exist between correlative volcanic and volcaniclastic rocks, we have used variations in phenocryst type, size, and abundance to identify up to three units in the Forest Reefs Volcanics (Fig. 2). Detailed measured sections, which incorporate this new compositionally based stratigraphic subdivision, were constructed from observations made from drill core logged systematically across the Cadia Valley.

We have applied relative and absolute dating techniques to samples of sedimentary and volcanic rocks in the Cadia Valley. U-Th-Pb isotope compositions of zircons were analyzed using excimer laser ablation-inductively coupled plasma-mass spectrometry (ELA-ICP-MS). Zircons were separated using conventional techniques. Optical photomicrographs and scanning electron microscope (SEM) cathodoluminescence were used to select least-fractured and inclusion-free zircons for analysis. Dating by ELA-ICP-MS followed a procedure described by Harris et al. (2004). Samples were ablated with a pulsed 193-lm ArF LambdaPhysik LPX 1201 UV excimer laser with constant 100-mJ energy, a repetition rate of 5 Hz, and a pit diameter of 32 μm. A mixed Ar-He (with minor H_2) carrier gas transported the ablated material from the sample cell into a flow homogenizer to an Agilent 7500 ICP-MS. Counts for ^{39}Si, ^{96}Zr, ^{31}P, ^{206}Pb, ^{207}Pb, ^{208}Pb, ^{232}Th, and ^{238}U and five rare earth elements (REEs) were collected in time-resolved mode.

Background was measured for 20 s with the laser turned off, and the sample measured for a further 40 s with the laser turned on, giving ~120 mass scans for a penetration depth of ~30 μm. Depth-dependent interelement and isotopic fractionation and instrumental mass bias of Pb, Th, and U (e.g., Hirata and Nesbitt, 1995; Horn et al., 2000) were corrected by reference to the standard zircon TEMORA and NIST610 silicate glass (Pearce et al., 1997; Black et al., 2004). Common Pb (the difference between the measured and expected ^{208}Pb/^{206}Pb)

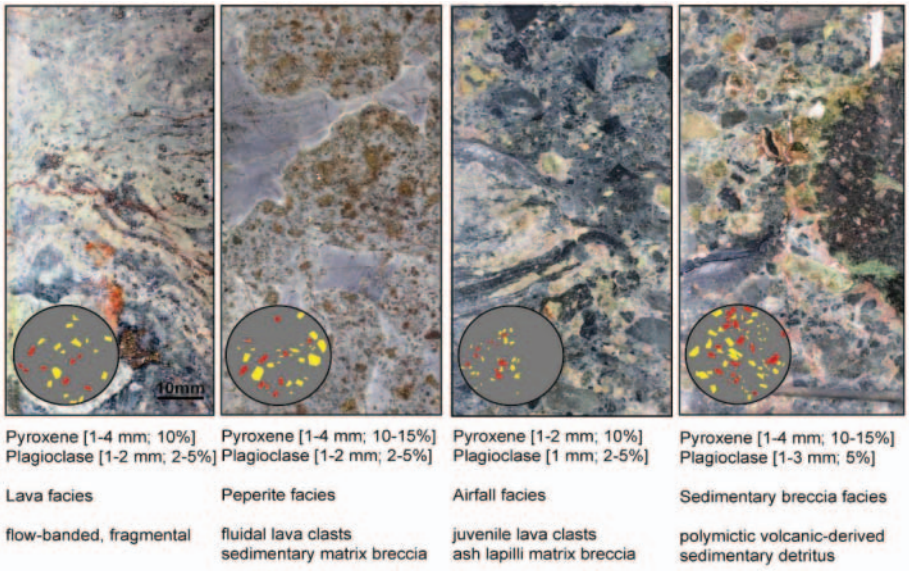

FIG. 2. Method for correlating volcanic stratigraphy through the Forest Reefs Volcanics. Shown here are correlative volcanic and volcaniclastic rocks that show identical phenocryst proportions (type, size, and abundance), irrespective of their mode of formation. This method can show that coherent facies (with same proportion of phenocrysts and, therefore, similar whole-rock geochemistry) intercalate lateral reworked equivalents that comprise dominant clasts of similar lava compositions. The same scale applies to all photographs. Ferromagnesian minerals are colored yellow. Feldspars are colored red.

was then subtracted, assuming a common Pb composition from the age-dependent Pb model of Cumming and Richards (1975). Assuming concordance, the $^{206}Pb/^{238}U$ ratios were then calculated by correcting for common Pb. Quoted uncertainties on individual samples are two times the standard uncertainty of corrected $^{206}Pb/^{238}U$ age for the selected portion of the population (see Appendix 1 for all analytical data).

Regional Geology

Ordovician rocks of the central Lachlan fold belt include several packages of arc-related calc-alkalic to shoshonitic volcanosedimentary sequences that were deposited over a 50-m.y. history of magmatism (Fig. 1; Glen et al., 1998; Crawford et al., 2007). Collectively, the Ordovician to Early Silurian sequences constitute the Macquarie Arc (Glen et al., 1998). Magmatic activity commenced in the Early Ordovician at the boundary between the Australian and proto-Pacific plates (Glen et al., 1998). Calc-alkaline and alkaline magmatism occurred episodically throughout the Ordovician associated with island-chain and deep-marine environments, consistent with the interpretation of the Macquarie Arc as a subduction-related island arc (Glen et al., 1998; Crawford et al., 2007; Glen et al., 2007; Percival and Glen, 2007).

The Ordovician to Early Silurian volcanosedimentary successions of the Cadia district occur in the Molong volcanic belt, one of the four segments of the dismembered Macquarie Arc, in the Eastern subprovince of the Lachlan Orogen (Fig. 1; Glen et al., 1998; Glen, 2005). Tectonic development of the arc is related to an early-formed W-dipping subduction zone (Glen et al., 1998). A more complicated setting is recognized in the Late Ordovician to Early Silurian with ongoing debate regarding the configuration of the arc (i.e., E- versus W-facing subduction; c.f. Crawford et al., 2007; Glen et al., 2007; Meffre et al., 2007; Percival and Glen, 2007; Squire and Crawford, 2007; Fergusson, 2009). Porphyry deposits formed immediately prior to and during accretion of the intraoceanic Macquarie Arc to Gondwana (i.e., the Late Ordovician to Early Silurian Benambran Orogeny; Cooke et al., 2007; Glen et al., 2007). At least two exhumation and deformation events occurred during this orogeny, i.e., ca. 443 Ma (late Bolindian to early Llandovery) and ca. 430 Ma (late Llandovery; Glen et al., 2007). Magmatism associated with porphyry deposit formation in the Cadia district (438–437 Ma; Wilson, 2003; Wilson et al., 2007a) occurred during a relaxation period after the first peak of deformation in the Benambran Orogeny (Glen et al., 2007).

The Ordovician Molong volcanic belt comprises multiple packages of volcanic and volcaniclastic rocks, including the Forest Reefs Volcanics. These are intercalated with turbiditic siltstones and sandstones, which are referred to as the Weemalla Formation (Pogson and Watkins, 1998). In describing the geology of the Cadia district, Wilson (2003) concluded that the Forest Reefs Volcanics is a thick (up to 3 km) pile of mafic and intermediate (andesitic and lesser basaltic and trachytic) volcanic and volcaniclastic rocks intruded by irregular mafic and silicic stocks, dikes, and sills. Regionally, the arc-related andesitic succession is dominated by thick sequences of volcanosedimentary breccias with volumetrically minor lavas (Squire, 2001). The volcaniclastic rocks conformably overlie fine-grained turbidites that are interpreted to have been deposited in a restricted sedimentary basin east-southeast of an arc-like volcanic succession (as represented by the Byng and Fairbridge Volcanics north and west of the Cadia district near Wellington and Cargo; Fig. 1; Crawford et al., 2007; Percival and Glen, 2007). A thicker apron of deep marine turbidites and fine-grained volcaniclastic rocks filled a more extensive basin that developed to the east of the Cadia district (Cabonne Group), which was flanked by the arc volcanic rocks of the Rockley-Gulgong volcanic belt.

District Geology and Stratigraphy

In the Cadia district, the preserved stratigraphy includes the Ordovician Weemalla Formation and Forest Reefs Volcanics (Figs. 3, 4). Silurian conglomerates, sandstones, and siltstones of the Waugoola Group unconformably overlie large portions of the Ordovician volcanosedimentary succession (Fig. 3; Washburn, 2008). Tertiary basalts of the Canobolas Volcanic Complex obscure these rocks to the north and east of the district (Fig. 3; Wellman and McDougall, 1974).

Weemalla Formation

The Weemalla Formation comprises laminated siltstone, and lesser siliceous siltstone and mudstone and feldspar-rich sandstone (Fig. 5). The fine- to medium-grained sandstones

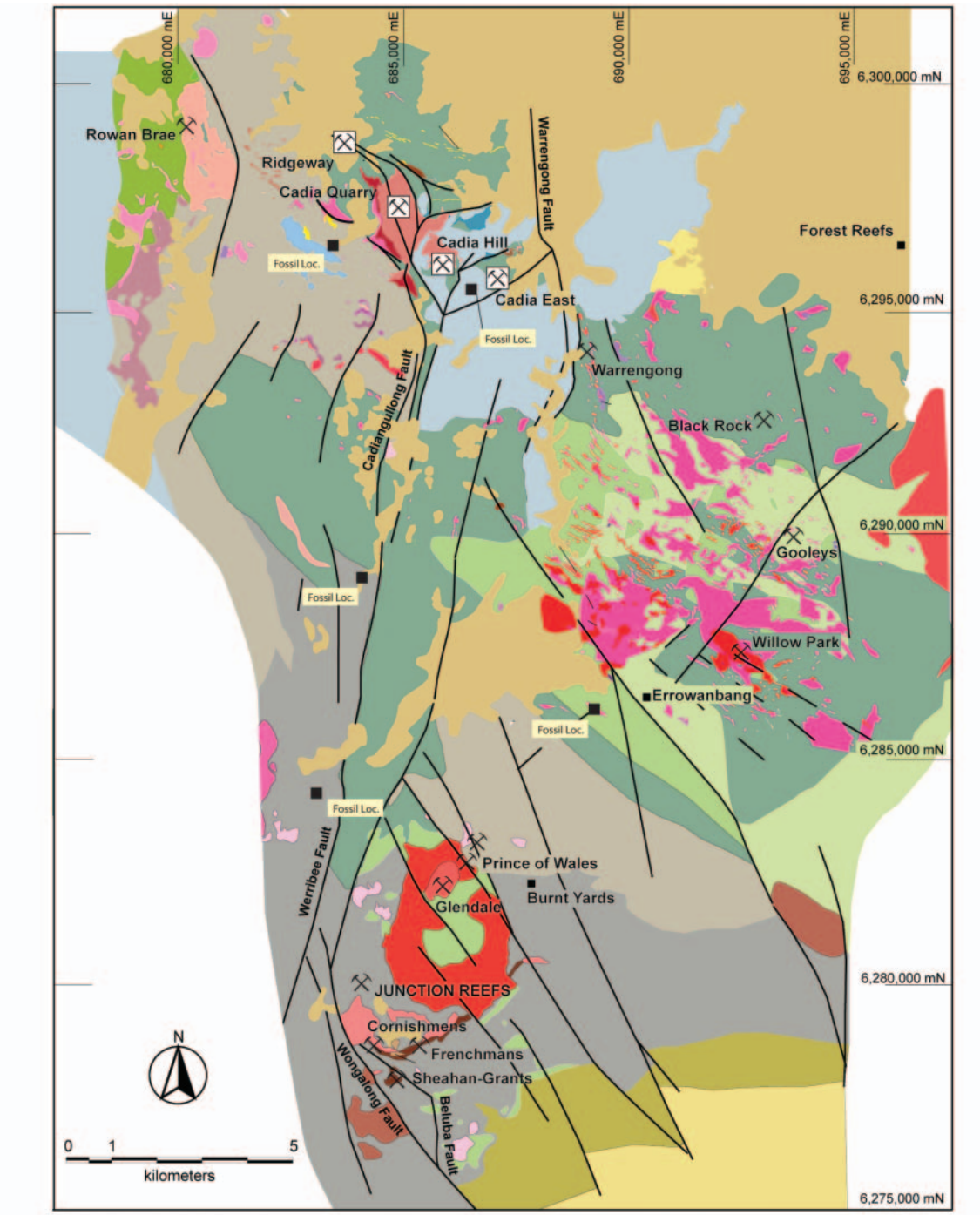

FIG. 3. Regional geologic map of the Cadia Valley and surrounding district (compiled from geologic maps produced during the 1990s; Homestake Mining and Newcrest Mining Ltd). Regionally, the Late Ordovician volcanic and volcaniclastic rocks interfinger with arc-derived feldspathic turbidite succession; Ea3 graptolites in turbidites (of the Weemalla Formation) are time equivalent to the Ea3 calcareous units of the Forest Reefs Volcanics.

are characterized by broken feldspar crystals (>90%) and rare quartz grains. Rare pyroxene-rich sandstones also occur. The Weemalla Formation is between 1,300 and 3,500 m thick, including ~500 m of pillow basalts, with lesser massive basalt and associated volcaniclastic rocks occurring at its base (Pogson and Watkins, 1998; Squire and Crawford, 2007). These intercalated basalts are locally the Mt. Pleasant Basalt Member.

The upper contact of the Weemalla Formation is gradational and intercalated with the overlying Forest Reef Volcanics (Fig. 6; Holliday et al., 2002; Wilson et al., 2003). This important stratigraphic feature is marked by an upsequence progression from laminated siltstone (with lesser siliceous siltstone and mudstone) to feldspathic sandstone and increasingly abundant volcanic-derived conglomerate. The feldspathic sandstone of the transitional sequence contains more feldspar crystals (~20%) and lithic fragments (~60%) than the black siltstones that characterize the Weemalla Formation. Equivalent sandstone and siltstone packages occur throughout the lowest parts of the Forest Reef Volcanics, suggesting that these units are in part contemporaneous and interfingered (cf. Zhen and Percival, 2004).

The Weemalla Formation contains a variety of paleofauna, including graptolites, conodonts, brachiopods, and minor fragmentary coral and trilobite remains. Conodonts from calcareous beds in the basal parts of the Weemalla Formation imply an early Darriwilian (Da2) age (Zhen and Percival, 2004) at about 465 Ma (Webby et al., 2004).

Sedimentation of the Weemalla Formation occurred in a proximal to distal wedge developed on the slopes of marine volcanic edifices (Pogson and Watkins, 1998). Based on the occurrence of thick, parallel-stratified beds of fine- to medium-grained sandstone that are laterally continuous over hundreds of meters, sedimentation is interpreted to have occurred in a broad, unconfined, deep water fan (e.g., Walker, 1978). The fine grain size, well-sorted nature, and the abundance of volcanic detritus are consistent with the Weemalla Formation being a distal sedimentary facies associated with submarine volcanic centers. Limestone fragments found in the basal parts of this formation imply that emergent edifices

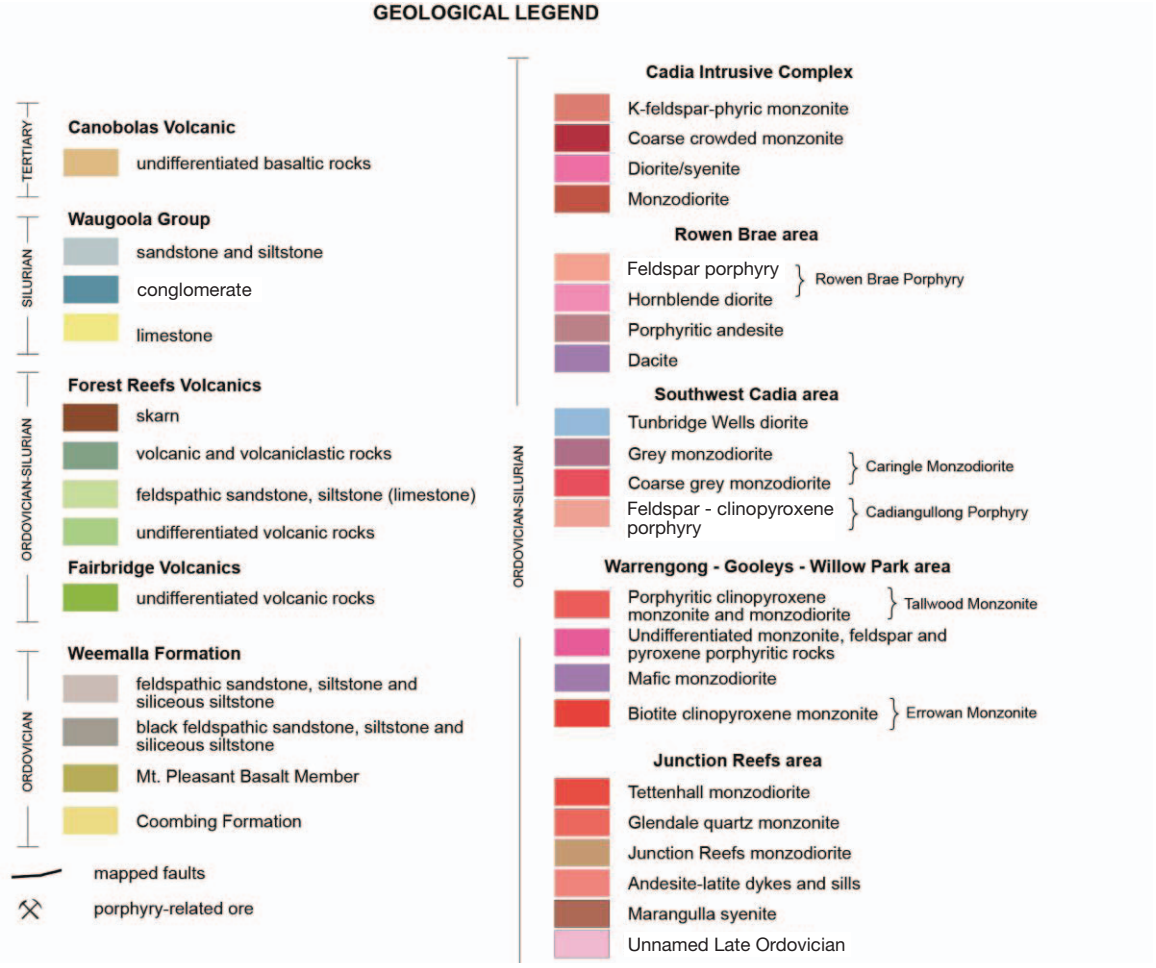

FIG. 3. *(Cont.)* Continuity of sedimentation between underlying deep marine basin deposits of the Weemalla Formation and Forest Reefs Volcanics, coupled with the predominance of sheet-like, laterally continuous debris flow and other coarse-grained sedimentary deposits, implies that volcanism and related sedimentation persisted in an active sedimentary basin. The most economically significant magmatic cycle in central New South Wales was associated with the latest Ordovician-earliest Silurian (Llandovery) intrusions, including the porphyry Au-Cu deposits of the Cadia Valley (444–439 Ma) and the Au-rich Junction Reef skarns. Sites of fossils important in correlating the turbidite sequence to the volcanic rocks are labeled "Fossil Loc."

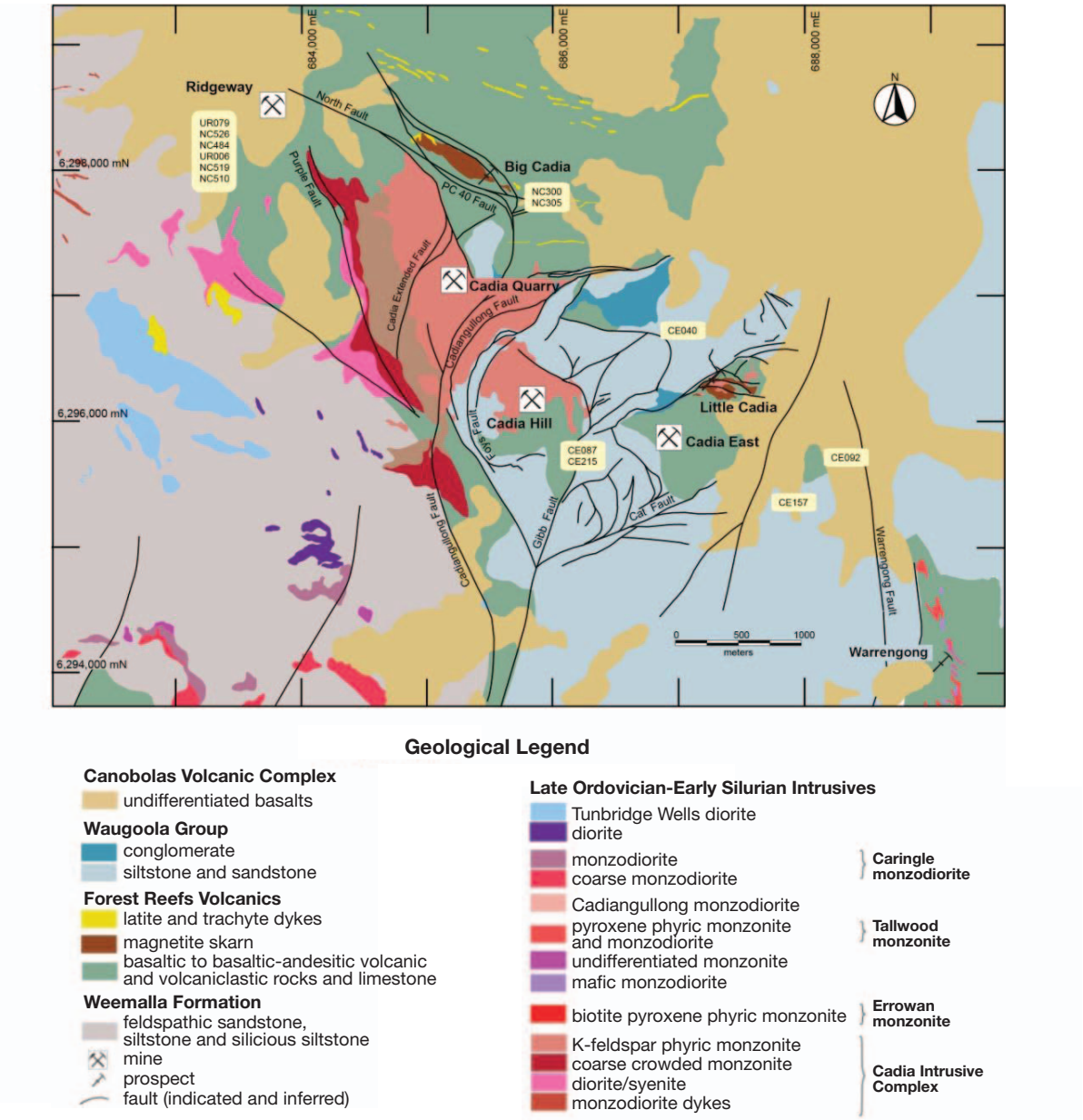

FIG. 4. District geology map of the Cadia Valley based on surface mapping by Newcrest Mining Ltd between 1997 and 2002. Geologic boundaries were further constrained using top-of-collar drill hole information (unpub. data, Newcrest Mining Ltd). Washburn (2008) mapped the Silurian cover rocks. Felsic intrusions and most of known ore deposits form a broad northwest trend that parallels the broader district trends evident in the previous map. Systematic logging of the drill holes across the Cadia Valley helps constrain the volcanic architecture. As has been shown elsewhere (Holliday et al., 2002; Wilson et al., 2003), the outcropping stratigraphy becomes younger to the east. The Forest Reefs Volcanics vary laterally and vertically in terms of eruptive style and composition of volcanism. At Ridgeway, a narrow zone (300 m) of porphyry-style alteration and mineralization occurs in and around multiphase monzonitic stocks. By contrast, the Cadia East deposit occupies a mineralized zone 2 km long, 600 m wide, and >1,500 m in vertical extent. Here, hydrothermal alteration and mineralization is lithologically controlled at surface, becoming more structurally controlled (as stockwork and sheeted vein arrays) at depth.

existed regionally at this time (Pogson and Watkins, 1998). Erosion of hydrothermal deposits (probably Darriwilian to Gisbornian in age, based on the available $^{40}Ar/^{39}Ar$ and fossil data) is implied in the abundance of detrital vein quartz in this unit (Packham et al., 1999). Similar depositional processes and environments persisted during deposition of the transitional sequence of the Forest Reef Volcanics.

Forest Reefs Volcanics

The Forest Reefs Volcanics are at least 2.5 km thick and include stratified clastic (volcanic-derived conglomerates and breccias, sandstone, and siltstone) and coherent lithofacies (Squire, 2001; Holliday et al., 2002; Wilson, 2003; Kitto, 2005). Volcanic rocks are high-K calc-alkaline to alkaline and vary in composition from basaltic to basaltic andesite,

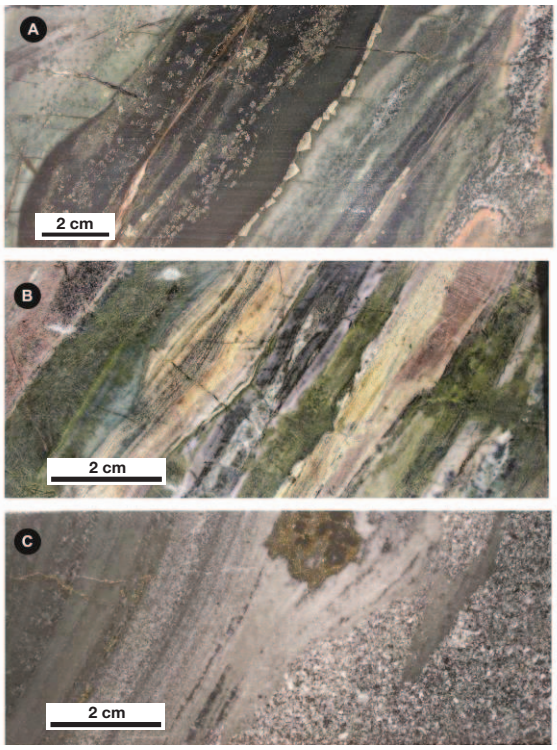

FIG. 5. Siltstone and sandstone of the Weemalla Formation and Forest Reefs Volcanics. A. Laminar interbeds of feldspathic sandstone and siltstone of the Weemalla Formation. B. Feldspathic sandstone, siltstone, and siliceous siltstone replaced by epidote-garnet-feldspar alteration, Weemalla Formation. C. Erosive base to a thin succession of feldspathic sandstone and siliceous siltstone intercalated within the Forest Reefs Volcanics.

andesite, and trachyandesite. The lowermost Forest Reefs Volcanics in and around the Ridgeway deposit include volcanic and volcaniclastic rocks that are more intermediate in composition (andesitic) compared to mafic (basaltic to basaltic andesitic) rocks in the upper parts of the stratigraphy to the east (Holliday et al., 2002). Studies by Squire (2001), Holliday et al. (2002), Wilson (2003), and Squire and McPhie (2007) recognized compositional variations in both the clastic and coherent facies of the volcanosedimentary succession and informally redefined the Forest Reefs Volcanics into an upper and lower subdivision, separated by an inferred, regionally extensive unconformity and/or fault (Squire and McPhie, 2007).

Age constraints: Absolute age determination of the basaltic andesitic volcanic rocks of the Forest Reefs Volcanics has proven difficult. No zircons were recovered from numerous Forest Reefs Volcanics samples processed as part of this study. Only one new U-Pb age was determined for volcaniclastic rocks (with distinct quartz-phyric dacitic clasts) in the basal parts of the stratigraphy. Zircons from this well-sorted polymictic sedimentary breccia (NC570, 1,200 m) yield a mean U-Pb age of 453.4 ± 3.6 Ma (n = 13; MSWD of 1.39), with a few clearly older zircons between 461 and 488 Ma (Appendix 1). These ages are similar to a previously reported detrital $^{40}Ar/^{39}Ar$ hornblende age (450.0 ± 1.2 Ma) from the sandstone and siltstone packages of the surrounding Weemalla Formation (GR. 688400 6274400, from C. Perkins, cited in Pogson and Watkins, 1998). On the basis of detrital zircon ages, the maximum deposition age for the lower Forest Reef Volcanics is 453 Ma, which overlaps the protracted deposition history of the Weemalla Formation from 465 to 450 Ma.

Fossil evidence implies that the Forest Reefs Volcanics were deposited after the Gisbornian (~460 Ma) and well before the Eastonian (450 Ma). Late Darriwillian to Gisbornian graptolites occur ~150 m above the Mt. Pleasant Basalt Member (Stevens, 1957), further constraining the onset of Forest Reefs Volcanics deposition. Conodont assemblages from calcareous units found in the Forest Reefs Volcanics at the Big and Little Cadia skarns are diagnostic of the Eastonian (Ea) 3 stage (~452 Ma; Packham et al., 1999). Cover rocks above this skarn mineralization further constrain the age of the Forest Reefs Volcanics. Siltstone and sandstone, with lesser limestone and conglomerate, of the Waugoola Group cover much of the Ordovician rocks (Fig. 7; Kitto, 2005; Washburn, 2008). Massive siltstone with thin interbeds of coarse-grained arkosic sandstone overlies basal conglomerates and limestones (Washburn, 2008). Fossil assemblages of these limestones imply that the rocks are largely Late Silurian (Packham et al., 1999; Rickards et al., 2001). Clasts of monzonite and skarn observed in the basal conglomerate imply uplift and exhumation of the Ordovician intrusive complexes prior to deposition of the Silurian cover rocks (Green, 1999; Washburn, 2008). The Silurian unconformity has cut down into high-temperature potassic (biotite) and sodic (albite-tourmaline-quartz) hydrothermal alteration of the Forest Reefs Volcanics through the central and eastern parts of the Cadia district.

Our study extracted age-significant fossils from two limestone horizons intersected in a single drill core that cuts the Waugoola Group and Forest Reefs Volcanics. Limestone from the Waugoola Group (drill hole CC003 at 125 m), immediately overlying the Forest Reefs Volcanics, displayed a cross section through the ventral valve of a smooth pentameride brachiopod that implies a Silurian age. By contrast, limestone taken from a succession of altered volcanic rocks in the upper parts of the Forest Reefs Volcanics (CC003 at 362.4 m) contains conodonts (including *Panderodus unicostatus*, *Oulodus* cf. *O. planus*, and several elements most likely referable to *Distomodus*) that have a definite Early Silurian aspect (Llandovery to Wenlock; Fig. 8).

Available chronologic data suggest the Forest Reefs Volcanics were deposited from the Ordovician through to the Early Silurian. The occurrence of monzonite fragments in some sedimentary breccias (Wilson, 2003; Kitto, 2005) that are intercalated with Early Silurian fossiliferous limestones represents evidence for degradation of the Forest Reefs Volcanics. This finding, combined with available absolute ages of crosscutting intrusions and associated hydrothermal alteration and mineralization (Wilson, 2003; Squire and McPhie, 2007; Wilson et al., 2007a), suggests that the uppermost preserved volcanosedimentary units were deposited synchronously with or immediately after the last known porphyry-related hydrothermal event in the Cadia Valley (437 ± 4 Ma; Wilson, 2003). This contrasts with the bulk of the Forest Reefs Volcanics that are clearly host rocks to the later hydrothermal alteration and mineralization.

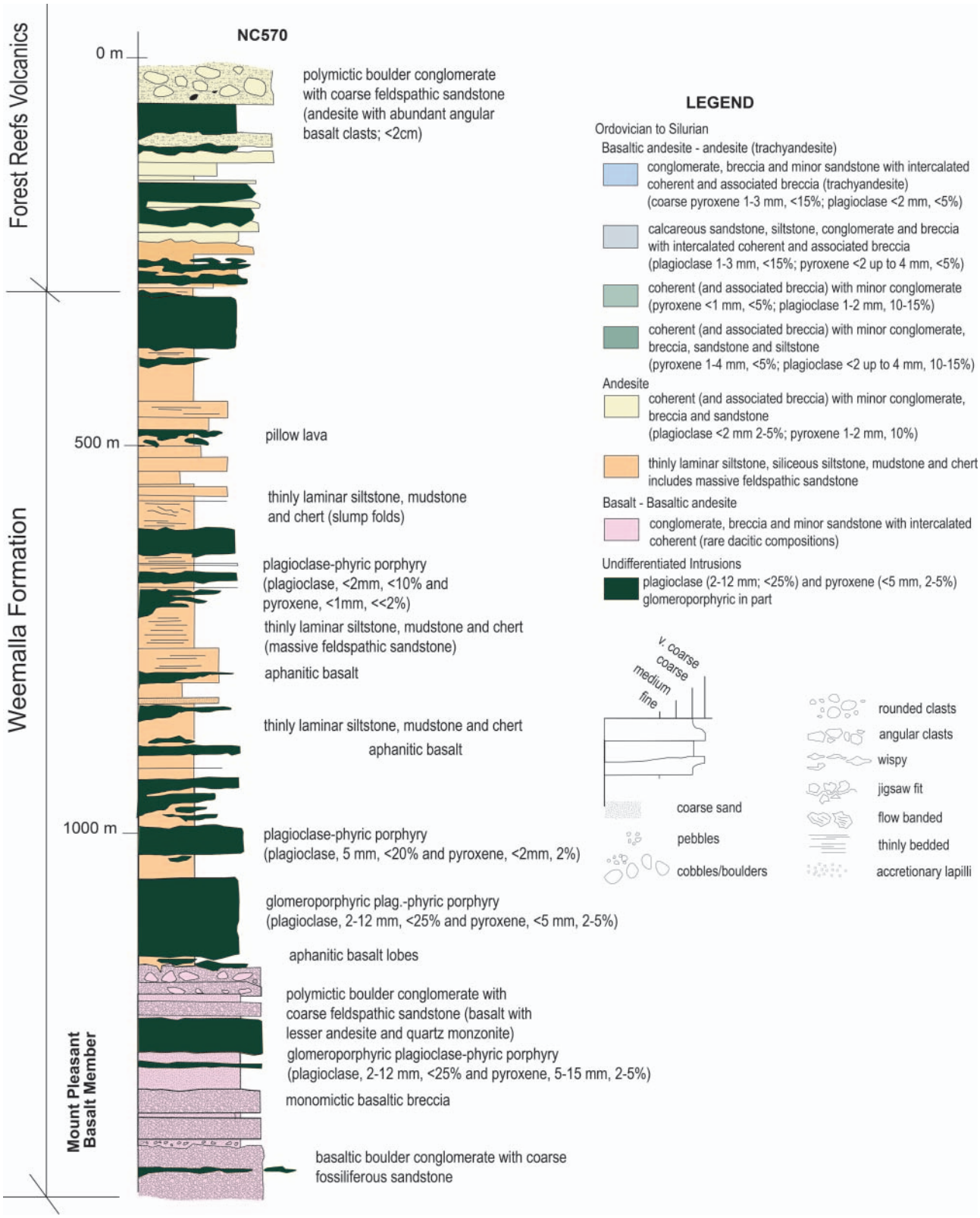

FIG. 6. Lithology variations across the transition from the Weemalla Formation (including the Mt. Pleasant Basalt) to the Forest Reefs Volcanics (drill hole NC570, located west of Ridgeway). New zircon U-Pb ages have been determined from volcaniclastic rocks of the Mt. Pleasant Basalt and yield a mean age of ca. 452 Ma (App. 1A). Intercalated fossiliferous carbonates imply that shallow marine conditions existed during effusive volcanism. Plag. = plagioclase. Rock unit legend used here applies to all graphical logs presented in this paper.

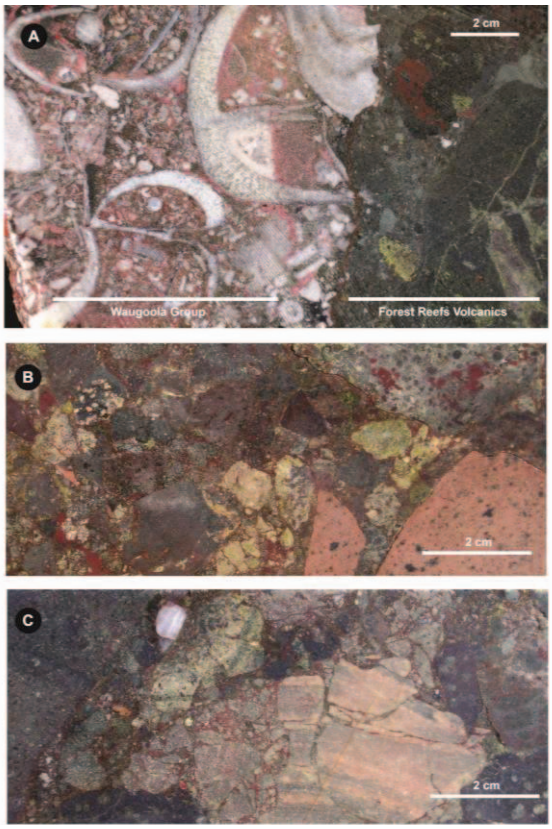

FIG. 7. The Silurian Waugoola Group. A. Unconformity between the fossiliferous limestone of the Late Silurian Waugoola Group and the altered volcaniclastic rocks of the Early Silurian-Late Ordovician Forest Reefs Volcanics. B. Polymictic sedimentary breccia comprising contrasting intrusive rocks, including aphanitic basalts and feldspar-phyric basaltic andesite. Epidote-altered clasts also occur. The sedimentary matrix in this breccia is altered by hematite-chlorite. C. Clasts of hydrothermal quartz veins and skarn occur in sedimentary breccias. Extracted fossils from these breccias are diagnostically Early Silurian. Limestones found at the top of the Forest Reefs Volcanics imply that accumulation of the volcanic-derived detritus occurred till the Early Silurian. A considerable thickness of volcanic and sedimentary overburden was removed (over 1 km) prior to the Early Silurian; exhumation resulted in the exposure of the Cadia Intrusive Complex, resulting in basin-fill material rich in monzonite clasts. Subsequent exhumation occurred prior to the deposition of the Silurian Waugoola Group (Wenlock to Ludlow, to Pridoli; Rickards et al., 2001; Rickards and Wright, 2004).

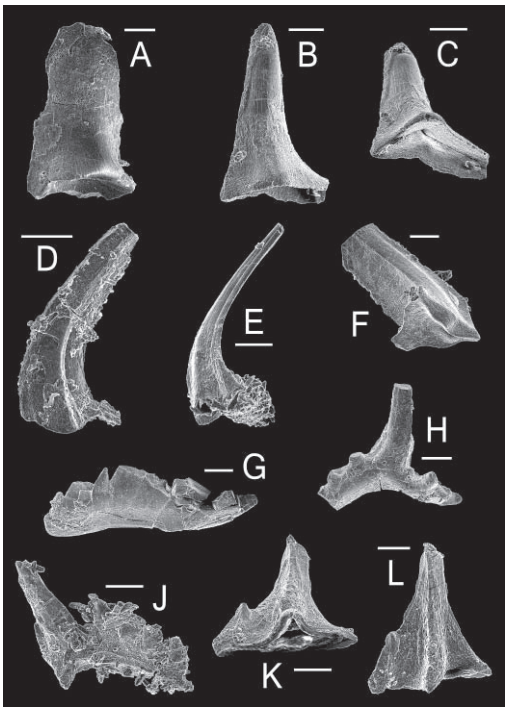

FIG. 8. Silurian conodonts from the uppermost parts of the Forest Reefs Volcanics (from drill hole CC003 at 362.4 m). A. Unidentified coniform element. B, C. *Distomodus* sp., M element, lateral and oblique basal views. D. *Panderodus unicostatus*. E. *Panderodus unicostatus*. F. *Distomodus*? sp., fragmentary element in oblique basal view. G. *Oulodus* cf. *O. planus*, fragmentary Pa element. H. *Oulodus* cf. *O. planus*, Pa element. J. *Oulodus* sp., M element. K, L. *Distomodus* sp., Pb? element, lateral and oblique basal views. Features of these conodonts are consistent with those considered Early Silurian (Llandovery-Wenlock) in age.

Structure: The volcanogenic sequences are gently tilted (<15°) and warped (plunging SE), but become steeper or upturned and folded close to major faults and intrusions. The volcanic succession is cut by numerous N- to NNW- and NE-trending faults, which are subsidiary structures of the prominent Werribee-Cadiangullong fault (Figs. 3, 4). Fabrics such as slickenside lineations and shears together with apparent stratigraphic offsets (10s–100s of meters) imply reverse (and, less commonly, normal) sense of movement on these faults. Displacements of up to 300 m have been measured, particularly in the juxtaposition of the Cadia Hill and Cadia East deposits (Holliday et al., 2002). Fault offsets are no greater than 600 m through Cadia Quarry based on displacement of sedimentary carbonate marker beds that flank the edge of the larger intrusive complex (Fig. 4). Some N- to NNW-trending faults appear to link to W- to NW-trending faults (e.g., the Purple and North faults at Ridgeway; Wilson et al., 2003).

WNW-oriented faults appear to have influenced deposition of the Forest Reef Volcanics. The presence of W-trending normal faults active during deposition of the Forest Reefs Volcanics is implied by stratigraphic thickness variations of 100s of meters in the Weemalla Formation, combined with irregular fault offsets of the Forest Reefs Volcanics. Localization of depocenters occurred along near-vertical W-trending structures. W-trending faults, such as the North fault, have been reactivated episodically with successive episodes of E-W shortening. The intersection of these W-trending faults with the more prominent N-trending fault zones is interpreted to have localized intrusions and porphyry mineralization at Cadia Hill and Cadia Quarry.

Alteration and mineralization: Fracture-controlled hydrothermal alteration and mineralization is typically centered on or in multiphase monzonitic stocks and dikes (Holliday et al., 2002; Wilson et al., 2003). Hydrothermal alteration assemblages are zoned from a central quartz (± biotite-K-feldspar-magnetite) core outward to potassic (K-feldspar-biotite ± magnetite) assemblages (e.g., Wilson et al., 2003, 2007b). Multiple stages of chlorite-epidote alteration (inner propylitic alteration) have overprinted the potassic alteration zone. Limited actinolite-magnetite-biotite (calc-potassic) alteration is also important at Ridgeway and, to a lesser extent, at Cadia East. An outer halo of sodic (albitic) and propylitic alteration (epidote-chlorite-albite-calcite-hematite) extends up to 1 km

away from Cadia East and, to a lesser extent, Ridgeway. Isolated magnetite-epidote (garnet-pyroxene) skarns are localized throughout the district (Green, 1999; Forster et al., 2004). Based on available fluid inclusion data, the depth of emplacement of the mineralized porphyries is interpreted to have been within 3 km of the paleosurface (Wilson et al., 2003).

Lithofacies of the Forest Reefs Volcanics and Weemalla Formation

The volcanic and volcaniclastic components of the Forest Reefs Volcanics are formed by effusive and explosive processes (Table 1). Irrespective of their compositions and stratigraphic positions, it is possible to recognize strata that share similar appearances and, by inference, processes of formation. Three common lithofacies associations occur in the Forest Reefs Volcanics, namely, primary volcanic, volcanosedimentary, and hypabyssal facies associations. Primary volcanic facies associations comprise facies that were generated only by volcanic eruptions—either explosive or effusive and/or shallow intrusions. This includes basalt and basaltic andesite lavas and associated lava breccias, hyaloclastite, and rare peperite. Lavas and their associated breccia facies, including deposits of reworked material, occur throughout the Forest Reefs Volcanics. Volcanosedimentary facies associations, including stratified sediment-matrix breccias, constitute up to 60% of the stratigraphy. Hypabyssal intrusions include dikes, sills, and stocks emplaced at relatively shallow depths (<3 km) and are mostly discordant to stratigraphy.

Primary volcanic facies associations

Subaqueous basaltic and basaltic andesite lavas: Thin (<20 m) intervals of basalt and basaltic andesite occur throughout the Weemalla Formation and parts of the Forest Reefs Volcanics. These units can be massive, flow banded, or fragmental. Rarely, stacked mafic lobate structures (pillows) occur with and without glassy margins. Intervals of this coherent

TABLE 1. Lithofacies of the Cadia Valley

Lithofacies	Composition	Characteristics
Subaqueous basaltic and basaltic andesite lavas	Basaltic, basaltic andesite to andesite	Thin (<20 m) lobes and sheets comprising massive or flow-banded coherent units; rare stacked mafic lobate structures (pillows); more andesitic units occur with isolated massive and flow-banded blocky fragments and/or fragmental domains; laterally continuous (>100 m) units conformable to bedding; nonerosive and concordant bases, with no disruption of sedimentary bedding
Coherent lava and in situ monomict lava breccia facies	Andesite and basaltic andesitic (trachyandesite)	Concordant coherent sheets (up to 25 m thick) with clast- and matrix-supported monomict breccia domains; restricted lateral continuity (less than a few hundred metres); irregular lobate domains (1–10 m across) of comparatively coherent lava surrounded by zones of tightly packed clast- to matrix-supported monomict breccia; angular clasts (2–5 cm in diameter) of dense and poorly vesicular volcanic fragments occur in crystal-rich volcanic sandstones; polygonal and blocky lava fragments (2–8 cm) occur as domains that show jigsaw-fit texture; flow banding occurs rarely in the coherent lava; units of the coherent lava and in situ monomict lava breccia facies form stacked, mound-like structures
Synsedimentary intrusions	Basaltic andesite (trachyandesite) and andesitic	Sheet-like coherent domains (up to 20 m thick) fragmented along the flat, bedding-parallel contacts; wispy lobes (up to 20 cm) and dissociated breccia zones occur along contacts; fragmental contacts (between 2 and 30 m thick) are monomict and nonstratified; clasts (2–5 cm in diameter, outsized up to 20 cm) are blocky, ragged (curviplanar), and equidimensional, poorly vesiculated; jig-saw fit textures are common; breccia matrix comprises fine-grained siltstone, feldspathic sandstone, and volcanogenic conglomerate
Phreatomagmatic ash-fall deposits		Ash- to lapilli-dominated bedded sequences; dominated by juvenile, poorly vesicular clasts (0.5–15 cm) set in a matrix of siltstone (rare mudstone) and sandstone (ash and lapilli), together with abundant broken crystals (<0.2–2 mm) and fiamme (0.2–5 cm); simple bed forms; accretionary lapilli (<10 mm in diameter) are conspicuously round to ovoid shaped and are typically size graded within beds
Laminated siltstone and volcanic sandstone		Laminated to massive siltstone, siliceous siltstone, and chert; associated beds of fine-grained crystal-rich (feldspar ± pyroxene) sandstone; massive bed forms are common with rare scours and cross beds; beds are laterally continuous over several tens of meters; rare interbedded volcanic-derived conglomerates
Volcanic lithic breccia and sandstone		Polymictic matrix-supported (less commonly clast supported) breccias dominated by angular to subrounded mafic to intermediate lava clasts with volcanic lithic sand matrix; single beds are typically thick (up to 30 m), massive to crudely graded; basal contacts are nonerosive; thick beds are massive, whereas thinner beds are crudely reverse graded, but are more commonly clast supported at or near their tops; single units are laterally continuous for several kilometers, maintaining nearly constant bed thickness, geometry, and composition throughout
Calcareous sandstone and siltstone		Calcareous sandstone and siltstone with siliceous siltstones and feldspathic sandstones; thinly laminated (<3 mm) to very thinly bedded (20 to 100 mm); calcareous units are up to 60 m thick and may be laterally continuous over tens of meters

facies occur as sheet-like and relatively laterally continuous (>100 m) units that are generally conformable to bedding.

Based on concordance with sedimentary bedding and glassy rinds on lava lobes and sheets, this basaltic and basaltic andesite lithofacies association is interpreted as subaqueous lavas (e.g., Hargreaves and Ayres, 1979). Massive and pillow basaltic lavas were probably emplaced in a variety of water depths, from shallow marine to deep oceanic environments. More intermediate compositions are flow banded and, in part, brecciated, consistent with more viscous flow. These subaqueous lava sequences include significant lava breccias, including those formed by quench fragmentation (hyaloclastites; e.g., Pichler, 1965; Kano, 1991).

Subaqueous pillow lavas are common to coherent facies of the Weemalla Formation (including the Mt. Pleasant Basalt Member; Squire, 2001), but are largely absent from the Forest Reefs Volcanics. Most subaqueous lavas found in the Forest Reefs Volcanics are more felsic in composition. These andesitic lavas are intimately associated with hyaloclastites. Some are associated with sediment-matrix lava breccias interpreted as peperite (e.g., White et al., 2000; Squire and McPhie, 2002).

Coherent lava and in situ monomict lava breccia facies: Throughout the Forest Reefs Volcanics, there are composite units of mixed coherent basaltic andesite-andesite with domains of clast- and matrix-supported monomict breccia. Single units are thick (<25 m) and sheet-like, with restricted lateral continuity (less than a few hundred meters). Layers are concordant with sedimentary bedding. Irregular lobate domains (1–10 m across) of coherent lava are surrounded by domains of tightly packed clast- to matrix-supported monomict breccia (Fig. 9). Crystal-rich volcanic sandstone supports angular clasts of dense and poorly vesicular volcanic fragments. Lava fragments are polygonal and blocky, with distinctly curviplanar edges (Figs. 9, 10). Groups of clasts show jigsaw-fit texture. Some splintery fragments occur. Units of the coherent lava and in situ monomict lava breccia facies form stacked, mound-like structures or sheet-like geometry. Individual lava facies can be compositionally distinct even though they occur adjacent to each other. Sedimentary breccias and crystal-rich sandstones are intercalated with and apparently flank the thick lavas facies. The occurrence of both coherent and brecciated lava material is interpreted as the subaqueous extrusion of lava and its subsequent partial disintegration by quench fragmentation processes (e.g., Dimroth et al., 1978; Bergh and Sigvaldason, 1991; Kano, 1991). The predominance of jigsaw-fit textures suggests that quench fragmentation occurred largely in situ. Clast- and matrix-supported monomict breccias are interpreted to be matrix-poor in situ hyaloclastite and matrix-rich hyaloclastite, respectively (Fig. 11). Eroded and reworked volcanic material laterally flanks the lavas. Sediment-matrix lava breccias (peperites) occur with the hyaloclastites (Fig. 11B). Facies associations

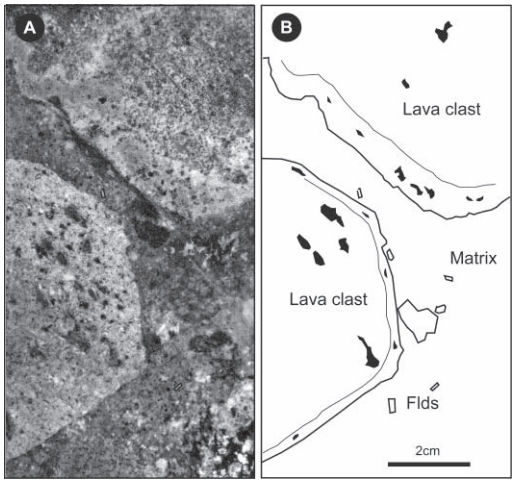

FIG. 10. Coherent lava and in situ monomictic lava breccia (drill hole CR063). A. Subangular clasts exhibiting jigsaw fit surrounded by matrix that is crystal rich and nearly identical to clast composition. B. Fine detail shows that single clasts exhibit a chilled margin rich in elongate amygdales that mirror the clast margin. Large (mm-scale) amygdales occur throughout the clasts. Clast and matrix are altered by pervasive albite replacement of groundmass and clast margins.

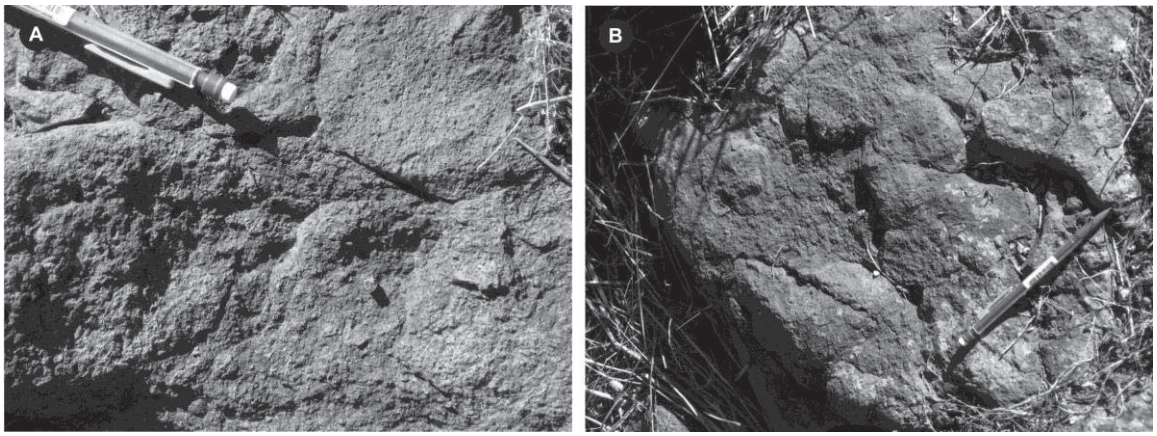

FIG. 9. Deposit characteristics of coherent lava and in situ monomictic lava breccia (Forest Reefs Volcanics). A. Clast-rich unit of finely vesicular juvenile clasts exhibiting distinct polygonal clast shapes. This clast-supported, tightly packed autoclastic breccia exhibits jigsaw-fit textures. B. Juvenile clasts can show irregular curviplanar and cuspate margins. In fine detail, the clast margins are distinctly ragged. Rare lobate (pillow-like) structures occur in more coherent domains. Pencil is 15 cm long (GR. 684468, 6298826).

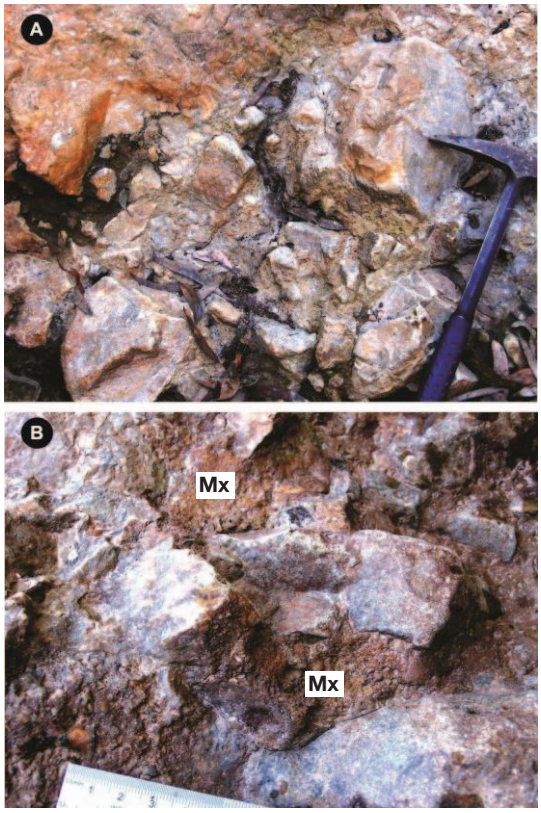

FIG. 11. Lava breccia. A. Lava lobe comprising numerous angular clasts that show good jigsaw-fit texture. This lobe is part of a larger sheet-like outcrop (interpreted as hyaloclastite). B. Domains of coarse-grained pebbly sandstone form the matrix to angular blocky breccias along the margins of this lava body (interpreted as peperitic margins). Pebbles can be seen in the lower left-hand side of the photograph. Field location GR. 686509, 6295870.

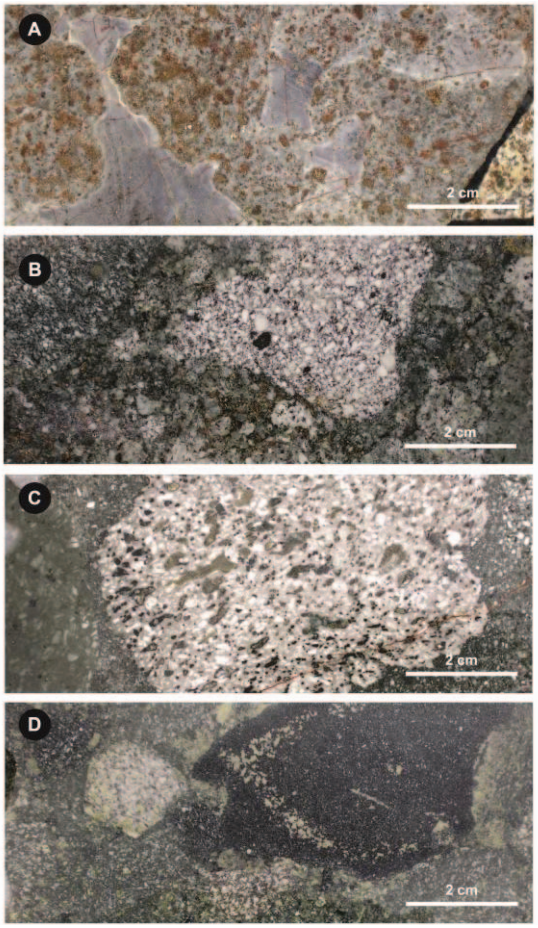

FIG. 12. Textural variations of volcanic and volcaniclastic rocks. A. Monomict angular breccia comprising feldspar-phyric andesite fragments with a matrix of coarse-grained lithic and feldspar sandstone (drill hole CR063). B. Irregular and wispy lava domains surrounded by embayments of siltstone and sandstone (interpreted as peperitic margin to thicker lava facies; drill hole NC592). C. Resedimented equivalent to the coherent lava and in situ monomictic lava breccia facies (drill hole CR063). Note the angular clasts exhibit distinctly ragged edges. Amygdales are broadly aligned. Incomplete amygdales are common along the broken clast edge. D. Polymictic nature of sedimentary breccias (including basaltic and andesitic compositions; drill hole CR063).

that comprise in situ hyaloclastite and coherent lavas form up to several hundred meters of combined thickness.

Synsedimentary intrusions: The Forest Reefs Volcanics contain a rare facies association of coherent andesite associated with blocky- and fluidal-clast breccia (Fig. 12A). The coherent facies ranges from small, lobate bodies (up to 20 m thick) to sheet-like units, fragmented along the flat, bedding-parallel contacts. Fragmental contacts, between 2 and 30 m thick, are typically monomict and nonstratified, comprising blocky, ragged clasts of poorly vesiculated coherent material. The breccia matrix comprises fine-grained siltstone, feldspathic sandstone, and volcanogenic conglomerate. These breccia facies occur on the upper and/or lower surface of concordant (sill-like) units.

The wispy lava lobes and local jigsaw-fit breccia in fine-grained sedimentary matrix, which are closely associated with coherent facies of the same composition, are interpreted to be fluidal- and blocky-clast peperite (e.g., White et al., 2000). These units formed by disintegration of magma that intruded unconsolidated sand and silt. The bedding-parallel geometry of the coherent facies indicates that they are sills emplaced into wet, unconsolidated substrates. Fluidal lava clasts imply ductile fragmentation of intermediate magma, compared to the more blocky breccias seen in the more mafic rocks (Squire and McPhie, 2002).

Phreatomagmatic ash-fall deposits: Thinly bedded (less than 3 m), laminated volcanic sandstones occur as distinct creamy white units in the upper parts of the Forest Reefs Volcanics at Cadia East (Fig. 13). This facies comprises juvenile (poorly vesicular) feldspar-phyric andesitic to dacitic clasts (0.5–15 cm) set in a matrix of siltstone (rare mudstone) and sandstone (ash, lapilli). Broken crystals of plagioclase and lesser pyroxene occur with wispy, cuspate fiamme. Bed forms are simple, either laminated or thickly bedded and normally graded. Vesicular blocks are concentrated in the base of single units. Numerous accretionary lapilli and mud lump-bearing ash layers are dispersed throughout the sequence.

The fine grain size, ash-rich nature, and presence of abundant accretionary lapilli and juvenile material indicate that these sandstones are tuffs formed by phreatomagmatic eruptions. Thin laminar, laterally continuous and normally graded beds, including accretionary lapilli-bearing ash layers, are

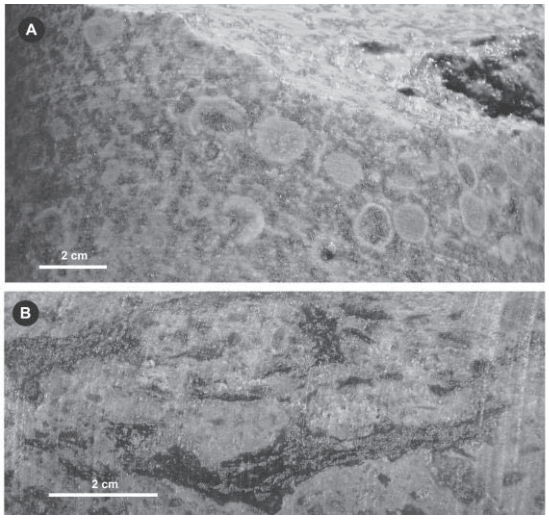

FIG. 13. Juvenile- and crystal-rich siltstone and sandstone. A. Accretionary lapilli and mud lump-bearing ash layer. The accretionary lapilli are conspicuously round to ovoid shaped. The presence of abundant accretionary lapilli and juvenile material indicates that these sandstones are tuffs formed from phreatomagmatic eruptions. B. Vesicular angular wispy juvenile clasts and cuspate fiamme set in crystal-rich mudstone and siltstone. These juvenile fragments with delicate wispy edges indicate hot, plastic emplacement.

interpreted to have been emplaced by fallout processes. The more silicic nature of the juvenile clasts implies that the causative explosive magmatic eruption came from a nearby basin margin or extrabasinal shallow-water or subaerial source (given the absence of known associated silicic lavas in the area). The absence of ballistic bombs suggests that these deposits are distal to their source.

It appears that the eruptive style was episodic and explosive in nature, as indicated by the high proportion of lapilli-sized pyroclasts, including juvenile clasts and fiamme, in the basal parts of the unit. The generally lithic poor and ash rich nature of the tuffs suggests magma interaction with surface water, producing fragmentation of vent and conduit facies (e.g., White, 1996). Ragged juvenile fiamme with delicate wispy edges indicate that lava blocks were hot and plastic. The abundance of whole and intact accretionary lapilli and the presence of graded ash and lapilli beds imply that these ash and lapilli tuffs were probably deposited in a subaerial environment.

Volcanosedimentary facies associations

Laminar siltstone and volcanic sandstone: Thin (~2 cm, up to 15 cm) beds of laminated to massive siltstone, siliceous siltstone, and chert are a distinctive feature of the Weemalla Formation and, to a lesser extent, of the Forest Reefs Volcanics (Fig. 5). Massive bed forms are common with rare scours and cross beds. Slump folds occur in thicker siltstone packages. Beds are laterally continuous over several tens of meters. Isolated rounded cobbles of igneous and volcanic detritus occur in coarse-grained lithic and feldspathic sandstones. Interbeds of volcanic-derived pebble conglomerates (up to 3 m thick) include 5% subangular to subrounded clasts (up to 10 cm) of flow-banded basaltic andesite and lesser sedimentary lithic clasts, including fragments of siltstone. Outsized clasts include boulders of monzonite. Conglomerates are matrix supported (comprising angular feldspar and pyroxene crystals) and poorly sorted. There are also rare black and gray mudstones and siliceous siltstones. Discrete packages of lithofacies define assemblages that are graded from thickly bedded fine- and coarse-grained feldspathic sandstones upward to sandstones with thin siltstone and chert partings. Rhythmically banded siltstone, siliceous siltstone, chert, and sandstone occur at the top of single sedimentary cycles, which are up to 40 m thick.

Laminar siltstone and volcanogenic sandstone facies of the Weemalla Formation are interpreted to be the product of suspension sedimentation of volcanic-derived (and limited biogenic) detritus from dilute turbidity currents. The fine grain size, thin laminae, and general lack of ripple cross laminations provide evidence for low energy conditions, particularly in the deposition of the more siliceous units. Grading from thickly bedded sandstone upward into siliceous siltstones and cherts is consistent with deposition from concentrated flows, where the upper sediments were deposited during residual low-density flows and trailing suspension (e.g., Squire, 2001). Slump folds most likely formed in unconsolidated, fine-grained sediments during down-slope movement. Squire (2001) suggested that such soft-sediment deformation implies rapid deposition on a low-angle slope. Observed lateral changes in bed thickness imply E-directed flow. The feldspathic nature of the sandstone implies minimal input from cratonic sources, rather than detritus derived directly from a developing volcanic arc (Pogson and Watkins, 1998). Laminar siltstone and siliceous siltstone interbeds throughout the Forest Reefs Volcanics imply that deposition from suspension settling of fine detritus persisted throughout the aggregation of the volcanosedimentary pile.

Volcanic lithic breccia and sandstone: Polymictic volcanic-derived breccias are dominated by angular to subrounded mafic to intermediate composition lava clasts with volcanic lithic sand matrix (Fig. 12B, C). Single beds are thick (up to 30 m), massive to crudely graded, and matrix supported (less commonly clast supported). Thicker beds (>15 m) generally lack internal structure or clast organization, while thinner beds (<5 m) exhibit variations in sorting and internal structure. Single units are laterally continuous for several kilometers, maintaining near constant bed thickness, geometry, and composition throughout (Squire, 2001; Wilson, 2003). Clasts typically have dimensions of 2 to 4 cm (locally up to 25 cm) and are entirely volcanic in origin, comprising different textural and compositional varieties of dark color mafic and intermediate lavas. Basalt and basaltic andesite clasts appear subordinate to porphyritic andesites (including plagioclase and pyroxene-phyric phases). Crystals of plagioclase and pyroxene and fine lithic fragments are set in a sand matrix.

The thick and massive bed character, polymictic nature, and coarse grain size of the breccias indicate deposition from concentrated sedimentary flows. Associated lithofacies and fossil assemblages imply a marine setting. Deposition from debris flows produced the thicker, massive, poorly sorted, and disorganized breccias. By contrast, the development of stratification, clast organization, and moderate sorting in some breccia beds is more consistent with deposition from concentrated density flows (Mulder and Alexander, 2002), comparable to hyperconcentrated flood flows that occur in subaerial

environments (e.g., Smith, 1986). Given the clast compositions, clast angularity, and coarse grain size of the sedimentary breccias, it is probable that some detritus was derived from local, primary volcanic facies. However, the well-sorted breccias with more rounded volcanic clasts are probably derived from more distal extrabasinal volcanic sources. The intervening thin cross-stratified siltstone and sandstone beds record deposition under lower sediment concentration conditions and turbulent suspension settling during the collapse of the debris flow.

The clast assemblage of the debris flow deposits includes primary volcanogenic and poorly consolidated primary volcaniclastic (i.e., resedimented syneruptive) detritus. The sheet-like and laterally continuous geometry of the volcanogenic sedimentary breccias is consistent with emplacement across a low-relief submarine plain (Squire, 2001; Wilson, 2003; Squire and McPhie, 2007). Submarine mud and debris flows have been shown to travel tens and even hundreds of kilometers on slopes of less than a few degrees (Elverhøi et al., 2005).

Calcareous sandstone and siltstone: Calcareous sandstone and siltstone occur throughout the Forest Reefs Volcanics and parts of the Weemalla Formation. These fine sandstones and siltstones comprise calcite, broken feldspars, and lesser volcanic-derived lithic fragments. The calcareous siltstones can be massive, but also occur as thinly laminated (<3 mm) to very thinly bedded (20–100 mm) units intercalated with siliceous siltstone and feldspathic sandstones. The calcareous units are up to 60 m thick and may be laterally continuous over tens of meters. Most calcareous units are fossiliferous and include conodonts, bryozoans, echinoderms, ostracods, radiolarians, brachiopods, nautiloids, calcareous algae, and coral (Pickett, 1992; Trotter and Webby, 1995; Packham et al., 1999; Zhen et al., 1999; this study).

Fossil assemblages suggest that the calcareous siltstones and sandstones were deposited in a shallow marine environment (e.g., Squire, 2001). The dominantly fine-grained nature suggests that most of the calcareous lithofacies were deposited by suspension settling. Interbedded feldspathic sandstones imply episodic influx of volcanic-derived detritus. Some volcanogenic detritus is coarse grained up to boulder sized, with a matrix of coarse-grained calcareous sandstone. The occurrence of near-complete fossils, including brachiopods with delicate overgrowths of calcareous algae, implies little to no mechanical transport and/or reworking of the sandstone matrix. Such findings imply proximity to both primary volcanic and sedimentary limestone sources.

Hypabyssal intrusions

Hypabyssal intrusions include dikes, sills, and stocks that crosscut other lithofacies (Holliday et al., 2002; Wilson et al., 2003). The intrusions range in composition from mafic to felsic and, rarely, ultramafic. Porphyritic textures are common, ranging from sparsely porphyritic to crystal crowded. Basalt and basaltic andesite intrusions are plagioclase- and/or pyroxene-phyric (Wilson et al., 2003). Andesite, trachyandesite, and monzonite intrusions are more commonly alkali feldspar-phyric with lesser plagioclase and rare hornblende. Some intrusions have plagioclase megacrysts up to 16 mm long, which are commonly twinned and zoned. Single intrusions of plagioclase megacrystic basaltic andesite are thick (100s of meters), sheet-like, and can extend laterally over several hundreds of meters or more. Narrow (20–50 m wide) trachyandesite (or latite) dikes have tabular (up to 8 mm × 1 mm) alkali feldspar crystals set in a cryptocrystalline groundmass.

There are coarser-grained (<12 mm) porphyritic and equigranular finger-like intrusions and large (up to km-scale) stocks. Some of these intrusions have undergone hydrothermal alteration and mineralization. Phenocrysts include clinopyroxene, plagioclase, and alkali feldspar set in a cryptocrystalline to fine-grained (<0.2 mm) groundmass. K-feldspar phenocrysts are distinctly tabular and/or square. Some feldspars are visibly zoned and inclusion rich. Bipyramidal quartz occurs in some of the monzonites. Other monzodiorite and monzonite intrusions are crowded with pyroxene and/or biotite. Subtle variations in phenocryst type, abundance, and size suggest that most of the monzonites are polyphase. Some intrusive contacts are diffuse or obscured by pervasive hydrothermal alteration assemblages inside the larger monzonite bodies (Holliday et al., 2002).

Subdivision of the Forest Reefs Volcanics

The compositional similarity that exists between lava and associated breccias, including lava autobreccias and their reworked equivalents, has helped in the recognition of laterally extensive stratigraphic markers. This complements existing studies that subdivided the Forest Reefs Volcanics using compositional differences and calcareous sedimentary units (Holliday et al., 2002; Wilson, 2003; Squire and McPhie, 2007). The fossiliferous nature of these sedimentary lithofacies has meant that time-equivalent deposits have been recognized; Late Ordovician conodonts have been extracted from skarn-bearing units at Big Cadia and Little Cadia (Packham et al., 1999). Additionally, calcareous marker beds that interfinger with compositionally distinct volcanic and volcaniclastic rocks have been identified.

The basal Forest Reefs Volcanics (up to 400 m thick) include volcanic and volcaniclastic material comprising evenly porphyritic andesite with fine-grained plagioclase (<2 mm; between 2 and 5%) with lesser hornblende (1–2 mm; 1%) and rare stubby pyroxene (1–2 mm; trace to 1%), and trace K-feldspar (1 mm) set in a cryptocrystalline to microcrystalline groundmass, referred to as hornblende-bearing plagioclase-phyric trachyandesite. Rare flow banding occurs in coherent units and breccia clasts. Feldspathic sandstone and conglomerates (volcanic-derived pebbles and cobbles) occur at the transition from the Weemalla Formation to the Forest Reefs Volcanics.

The lower parts of the Forest Reefs Volcanics preserved around Ridgeway include evenly porphyritic trachyandesite with fine-grained plagioclase (1–2 mm up to 4 mm; 10–15% up to 25%; Figure 14). The trachyandesite also contains fine stubby pyroxene (up to 1 mm, rarely up to 4 mm; <5%) and rare K-feldspar. Two compositional variants further subdivide this unit; a finer-grained pyroxene-phyric trachyandesite in the lower parts, and coarser-grained varieties higher in the stratigraphy (Fig. 14). The base (up to 150 m) of this stratigraphic subdivision is marked by laterally extensive, thinly bedded carbonate and feldspathic sandstone that transition upward to thickly bedded volcanic-derived conglomerate. Associated

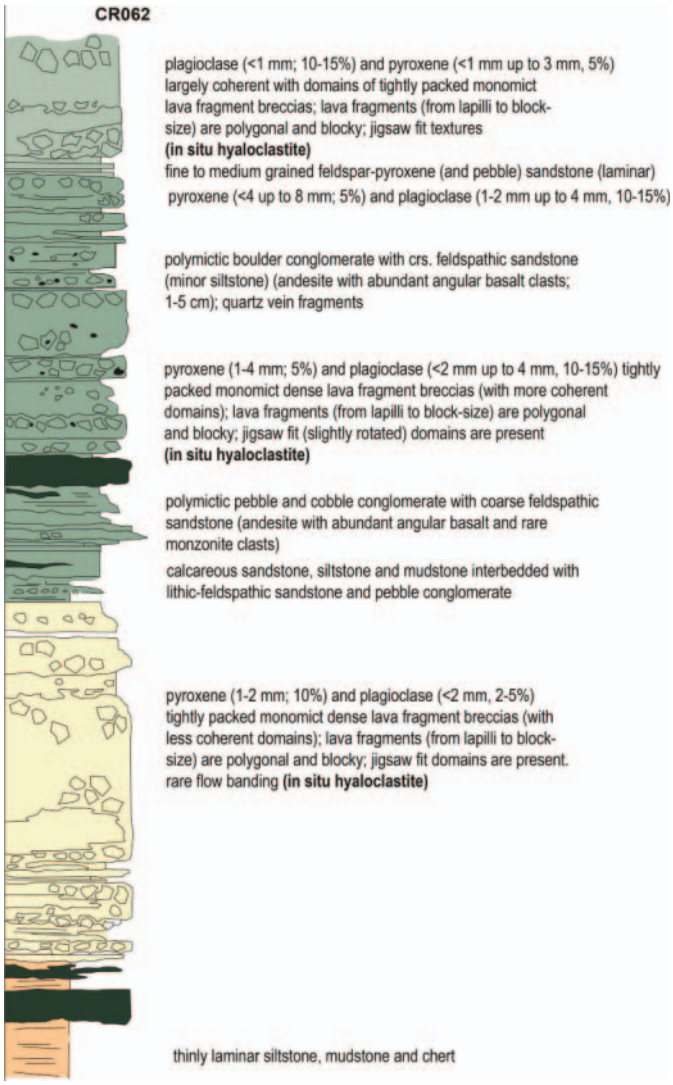

FIG. 14. Graphic log showing lithology variation in the basal parts of the Forest Reefs Volcanics. Hyaloclastites overlap and intercalate fine-grained feldspathic turbidites. Lava compositions change upsequence.

lavas are 10 to 30 m, rarely up to 50 m, thick. Intercalated sandstone and sedimentary breccias (up to 80 m thick) include polymictic boulder conglomerates (andesite compositions with lesser basalt and rare monzonite clasts) with coarse-grained feldspathic sandstone and minor siltstone.

Upper parts of the Forest Reefs Volcanics comprise crowded to evenly porphyritic basaltic andesite (trachyandesite) lava compositions with stubby plagioclase (1–3 mm; <15%) coexisting with pyroxene (up to 4 mm; 5–10%). Two compositional variants further subdivide this unit: a finer-grained pyroxene-phyric trachyandesite that occurs in the lower parts, and coarser-grained varieties that occur higher up (Fig. 13). Basaltic andesite and andesite lava units (10–30 m thick) include lava fragment breccias (with coherent domains). Lava breccia with sedimentary matrix is also common. Polymictic breccias and conglomerate (rich in basaltic clasts) are intercalated with the volumetrically more abundant lava. There are pyroxene- and feldspar-rich sandstones intercalated with the lavas. The upper parts of the sequence comprise laterally extensive laminar crystal-rich volcanic sandstone rich in fiamme, and locally contain mud lumps and a predominance of basaltic sedimentary detritus.

Facies Distribution and Implications for Basin Architecture

The spatial distribution of the rock types described above incorporates the Weemalla Formation (and Mt. Pleasant Basalt Member) and the Forest Reefs Volcanics (Figs. 6, 14). These subdivisions differ in terms of eruptive styles and volcanic compositions, along with sedimentary source and depositional setting. The lower stratigraphic subdivision of the Weemalla Formation is dominated by laminar siltstones, siliceous siltstone, cherts, and volcanogenic sandstones. These sedimentary units are intercalated with basalt and basaltic andesite lavas, synsedimentary sills, and volumetrically minor calcareous sandstones and volcanogenic sedimentary breccias and sandstones (Fig. 6). The Forest Reefs Volcanics largely comprise thick sequences of mafic to intermediate volcanic-derived sedimentary breccias with lesser conglomerate, sandstone, and siltstone, intercalated with basaltic andesite and andesite lavas, peperite, and hyaloclastite (Figs. 12, 13). Isolated air-fall deposits have also been recognized. The entire volcanosedimentary succession has been cut by mafic to felsic dikes and stocks.

In the Cadia district, the minimum observed thickness of the Weemalla Formation is 800 m, of which at least 500 m includes laminar siltstones and feldspathic sandstones. The predominance of fine-grained volcanogenic sedimentary interbeds, including deposits formed from suspension sedimentation and dilute turbidity flows, suggests the persistence of a marine sedimentary basin throughout the accumulation of the Weemalla Formation. The sheet-like and laterally continuous geometry of the laminar siltstones and feldspathic sandstone horizons is consistent with deposition across a low-relief submarine plain. Abundant feldspathic sandstones and the lack of quartz-rich flysch imply minimal cratonic input, in contrast to the Ordovician siliciclastic turbidites that are more commonly found throughout the Lachlan fold belt (e.g., Fergusson and Colquhoun, 1996). Rather, the thick package of volcanogenic detritus accumulated in a sedimentary basin on the flank of an eroding volcanic arc.

The Mt. Pleasant Basalt Member within the Weemalla Formation includes small-volume lavas, peperites, and sills intercalated with volumetrically minor calcareous sandstones and volcanogenic sedimentary breccias and sandstones. The basaltic lavas may have formed as several small low-relief submarine lava fields, or as parts of more substantial lava shield volcanoes (Squire and McPhie, 2007). The low-relief nature is inferred from the thin (up to 50 m) single lava flows scattered throughout most of the Weemalla Formation. More significant intrabasinal topography is implicit in the thickly stacked lava sequences (up to a few hundred meters) that crop out south of the Cadia Valley (Squire and McPhie, 2007). The lavas and intrusions of the lower stratigraphic subdivision are petrographically similar to clasts in the sedimentary breccias, and are therefore representative of the volcanic sources to these breccias. Exotic lithic clasts include quartz-eye dacite inferred to be sourced

more regionally (e.g., Cargo Volcanics; Simpson et al., 2007). The sedimentary units are therefore interpreted to have both intrabasinal volcanic and extrabasinal basement sources.

The transition from the Weemalla Formation to the Mt. Pleasant Basalt Member is conformable, indicating the widespread initiation of mafic volcanism across the submarine plain (Squire and McPhie, 2007; Fig. 6). The thin transitional sequence of mixed carbonate and basaltic volcanic provenance between the upper parts of the Mt. Pleasant Basaltic Member and the Weemalla Formation indicates that mafic volcanism constructed edifices that became increasingly shallow marine (implicit in the observed fauna assemblages). Overlapping fine-grained feldspathic turbidites (in part intercalated with less common basaltic lavas) suggest rapid subsidence during the earliest effusive basaltic volcanism in the Cadia Valley. No unconformities or angular disconformities are apparent in the siltstones and sandstones of the Weemalla Formation (cf. Squire and McPhie, 2007).

Volcanosedimentary rocks of the Forest Reefs Volcanics conformably overlie and interfinger with the Weemalla Formation (Holliday et al., 2002; Wilson et al., 2003). The transition is marked by the appearance of massive polymict volcanic-derived breccias (up to 2 m thick), with lesser lava facies (including feldspar-phyric hyaloclastites). Sills and dikes have obscured the transition locally (Wilson et al., 2003). Bedded (cm- to m-scale) lithic sandstones and pebble conglomerates mark the switch from turbiditic sedimentation to more proximal volcanic-derived sedimentation in some localities.

Volcanism that occurred during aggradation of the Forest Reefs Volcanics was more evolved (typically andesitic with lesser basaltic andesite and trachyandesite compositions) than the basaltic lavas that characterize the Weemalla Formation. Effusive eruptions appear to have occurred from multiple vents, producing thickly stacked lava sequences and cryptodome complexes (e.g., Batiza and White, 2000). The complex juxtaposition of lavas, hyaloclastites, and peperites (proximal) with resedimented fine-grained equivalents (distal facies) and other sedimentary breccias implies that some cryptodomes were only partially extrusive. Intermediate lobes are intercalated with more mafic lavas (Figs. 6, 14, 15). The occurrence of shallow marine fossils with the subaerial phreatomagmatic deposits (e.g., accretionary lapilli tuffs) near the upper parts of the stratigraphy implies that the volcanic center became emergent locally.

The complex interstratification of primary and reworked volcanic facies with more distal turbiditic facies is consistent with volcanism occurring in an overall low relief terrain (Fig. 16). This implies the existence of a large marine basin during volcanism at Cadia. Sedimentation styles change upsequence to the point where there is more evidence for restricted sedimentary environments. This is reflected in upsequence variation of sedimentary deposits, ranging from siltstones and feldspathic sandstones, carbonate sandstones, and pebble conglomerates to debris flow deposits with boulder-sized clasts. The occurrence of angular (including tabular) clasts of siltstone and siliceous siltstone (identical to those that compose the Weemalla Formation) in conglomerates and breccias in the upper assemblage suggests that lithified turbiditic basement rocks were being reworked and that positive topography was being constructed locally during the deposition of the Forest Reefs Volcanics.

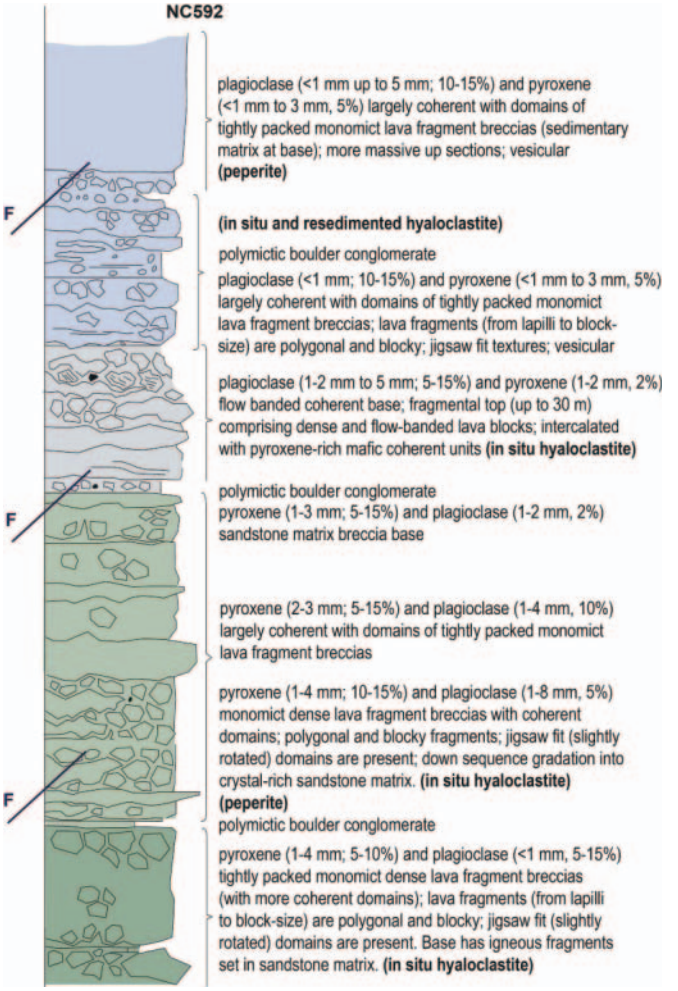

FIG. 15. Graphic log showing lithology variation through largely coherent facies in the uppermost parts of the Forest Reefs Volcanics. Lateral equivalents to the lavas occurring at the top of this section include air-fall deposits that record sustained phreatomagmatic eruptions (drill hole NC582, east of Cadia East).

Spatial relationships of observed volcanic and sedimentary facies, combined with stratigraphic thickening, show that volcanic detritus accumulated in subbasins between volcanic landforms at Cadia (Fox et al., 2009; Cooke et al., 2010). At Ridgeway, basin-fill facies grade laterally from thick (up to 200 m) coarse-grained volcanic breccias and conglomerates through mixed breccia and sandstone facies toward a thin (~50 m) sequence of finer-grained sandstones and siltstones. This package of rock is wedge shaped across 600 m, where the thickest point is immediately adjacent to a major NNE-trending fault. Up to 300 m of sedimentary detritus occurs in the center of NW-trending basins; laterally, the basin-fill stratigraphy thins (to <20 m) onto volcanic basement that flanks the elongate NW-oriented basins. Cryptodomes and thick lava sequences are localized along the margins of these basins. The monzonite intrusive complex related to mineralization at Ridgeway is centered in this sedimentary basin.

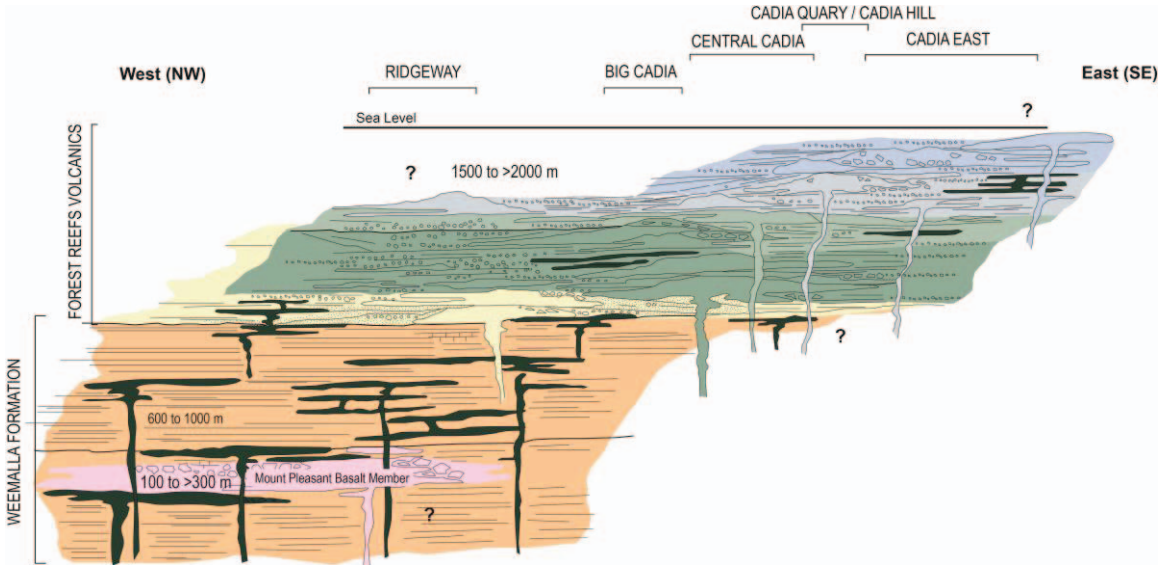

FIG. 16. Schematic representation of the volcanic facies architecture of the Cadia district showing the position of several key geographic locations, including the Ridgeway and Cadia East ore deposits. The paleogeography shown is that inferred for the Late Ordovician, immediately prior to the emplacement of the ore-forming intrusions. The preserved stratigraphy records an evolution from effusive to explosive volcanism. Available chronologic data suggests the Forest Reefs Volcanics were deposited from the Ordovician through to the Early Silurian.

Conclusions

Porphyry ore deposits are commonly hosted in volcanic successions. Rarely are these volcanic rocks truly coeval with ore-related magmatism. Despite this, understanding the volcanic architecture can be vital to better understanding what geologic elements acted to localize hydrothermal alteration in porphyry ore deposits and the surrounding district (e.g., Cooke et al., 2007). The recognition that volcanosedimentary basins are an important setting for porphyry deposits has implications for hydrological models of fluid flow in these large-volume hydrothermal systems. In such an environment, the near-surface facies architecture profoundly affects the nature of hydrothermal fluid flow and subsequent alteration and mineralization. Nearly identical settings have been documented for the distinctive Fe oxide Cu-Au (IOCG) deposits (e.g., Barton and Johnson, 1996; Groves et al., 2010), the geology of which is remarkably similar to that of the Cadia alkalic porphyry Au-Cu deposits.

In the Cadia district, the nature and distribution of volcanic and sedimentary rocks reveal that the cluster of the Au-rich porphyry deposits was emplaced into a marine volcanosedimentary basin. The transition from the Weemalla Formation to Forest Reefs Volcanics records a major provenance change from more proximal extra- and intrabasinal mafic to intermediate volcanic sources. Volcanogenic sedimentation overwhelmed the fine-grained sedimentary component that characterized much of the Weemalla Formation. Volcanism in the Cadia district, preserved in the Forest Reefs Volcanics, evolved as a relatively low relief, multiple-vent submarine volcanic complex. The vents comprised mafic to intermediate lava flows, cryptodomes, and subvolcanic intrusions (dikes and sills). Stacked lava sequences, including hyaloclastites, massive lavas, and their reworked equivalents, are up to 1 km thick, forming significant intrabasinal topography. Erosion and irregular unconformities (including one that is regionally extensive) developed late in the basin history. The stratigraphy suggests a progressively shallowing basin and evolving depositional environment throughout the Ordovician to the earliest Silurian. Explosive volcanism occurred during the late stages of Forest Reefs Volcanics deposition, resulting from sustained subaerial phreatomagmatic eruptions. Good textural preservation of the air-fall deposits, combined with coexisting shallow-water faunal assemblages, implies that volcanism became emergent locally. Continuity of sedimentation between underlying deep marine basin deposits of the Weemalla Formation and Forest Reefs Volcanics, coupled with the predominance of sheet-like, laterally continuous debris flow and other coarse-grained sedimentary deposits, implies that volcanism and related sedimentation persisted in an active sedimentary basin that was part of a larger basin system at the margins of an oceanic island arc. More regionally, basin-fill stratigraphy (e.g., Oakdale and Cheeseman Creek Formation; Percival and Glen, 2007) extends over 100 km north and south of the Cadia district.

Deposition of the Forest Reefs Volcanics spanned the Late Ordovician to Early Silurian. Emplacement of the Au-rich porphyry deposits occurred in an evolving marine basin with episodic intrabasinal magmatism. Formation in such an environment acted to localize the porphyry-related ore deposits; permeable horizons, including basin-fill successions, host regionally extensive (km-scale) Cu-Au mineralization and related hydrothermal alteration assemblages (Holliday et al., 2002; Wilson et al., 2007a; Fox et al., 2009). In the upper parts of Cadia East, volcanic and volcaniclastic facies architecture profoundly affected the nature of hydrothermal fluid flow and subsequent alteration; fluid flow of magmatic fluids into permeable strata at shallow levels produced disseminated replacement-style Cu-Au mineralization and km-scale

pervasive hydrothermal alteration (Fox et al., 2009). As such, this finding suggests that hydrological models of fluid flow in porphyry systems need to account for basin architecture.

Acknowledgments

Work presented here forms part of a collaborative research funded by Newcrest Mining Limited and the ARC Centre of Excellence in Ore Deposits (CODES). Newcrest Mining Limited is thanked for ongoing financial and logistical support and access to the Cadia Valley Operations. We are indebted to the numerous Newcrest exploration and mine geologists who shared their knowledge, which ultimately led to the success of this study. We greatly appreciate the contributions of John Holliday, Geoff Smart, Stuart Hayward, Dean Fredrickson, Joel Kitto, and Anne Eastward, whose knowledge guided our work. Malissa Washburn and Liezl Cuison are thanked for their input and lively discussions. Noel White is thanked for reviewing earlier versions of the manuscript. We acknowledge the valuable insights and critical reviews given by Alan Wilson and Thomas Bissig. Thanks to Ross Large and the staff at the ARC Centre of Excellence in Ore Deposits, who helped in the completion of this project. Ian Percival publishes with permission of the Executive Director, NSW Resources and Energy.

REFERENCES

Barton, M.D., and Johnson, D.A., 1996, Evaporitic source model for igneous related Fe oxide-(REE-Cu-Au-Au) mineralization: Geology, v. 24, p. 259–262.

Batiza, R., and White, J.D., 2000, Submarine lavas and hyaloclastite, *in* Sigurdsson, H., ed., Encyclopedia of Volcanoes: San Diego, Academic Press, p. 361–381.

Bergh, S.G., and Sigvaldason, G.E., 1991, Pleistocene mass-flow deposits of basaltic hyaloclastite on a shallow submarine shelf, south Iceland: Bulletin of Volcanology, v. 53, p. 597–611.

Black, L.P., Kamo, S.L., Allen, C.M., Davis, D.W., Aleinikoff, J.N., Valley, J.W., Mundil, R., Campbell, I.H., Korsch, R.J., Williams, I.S., and Foudoulis, C., 2004, Improved $^{206}Pb/^{238}U$ microprobe geochronology by the monitoring of a trace element related matrix effect; SHRIMP, IC-D-TIMS, ELA-ICP-MS and oxygen isotope documentation of a series of zircon standards: Chemical Geology, v. 205, p. 115–140.

Blevin, P.L., 2002, The petrographic and compositional character of variably K-enriched magmatic suites associated with Ordovician porphyry Cu-Au mineralisation in the Lachlan fold belt, Australia: Mineralium Deposita, v. 37, p. 87–99.

Cooke, D.R., Harris, A.C., Braxton, D.P., and Simpson, K.A., 2007, Basins, breccias and basement—diverse settings for porphyry deposits: Society for Geology Applied to Ore Deposits (SGA), 9th Biennial SGA Meeting, Dublin, Ireland, 20–23 August 2007, Proceedings, p. 395–398.

Cooke, D.R., Harris, A.C., Fox, N., Cuison, A., Tosdal, R.M., Groome, M., Percival, I.G., Dunham, P.D., Collett, D., Holliday, J., and Allen, C.M., 2010, Architectural controls on Paleozoic porphyry gold-copper mineralisation in the Cadia Valley, NSW: Canberra, Geological Society of Australia, 2010 Australian Earth Sciences Convention, Abstract no. 98, p. 175.

Crawford, A.J., Glen, R.A., Cooke, D.R., and Percival, I.G., 2007, Geological evolution and metallogenesis of the Ordovician Macquarie Arc, Lachlan orogen, New South Wales: Australian Journal of Earth Sciences, v. 54 , p. 137–479.

Cumming, G.L., and Richards, J.R., 1975, Ore lead isotope ratios in a continuously changing earth: Earth and Planetary Science Letters, v. 28, p. 155–171.

Dimroth, E., Cousineau, P., Leduc, M., and Sanschagrin, Y., 1978, Structure and organisation of Archean basalt flows, Rouyn-Noranda area, Quebec, Canada: Canadian Journal of Earth Science, v. 15, p. 902–918.

Elverhøi, A., Issler, D., De Blasio, F.V., Ilstad, T., Harbitz, C.B., and Gauer, P., 2005, Emerging insights into the dynamics of submarine debris flows: Natural Hazards and Earth System Sciences, v. 5, p. 633–648.

Fergusson, C.L., 2009, Tectonic evolution of the Ordovician Macquarie Arc, central New South Wales: Arguments for subduction polarity and anticlockwise rotation: Australian Journal of Earth Science, v. 56, p. 179–193.

Fergusson, C.L., and Colquhoun, G.P., 1996, Early Palaeozoic quartz turbidite fan and volcaniclastic apron, Mudgee district, northeastern Lachlan fold belt, New South Wales: Australian Journal of Earth Sciences, v. 43, p. 497–507.

Forster, D.B., Seccombe, P.K., and Phillips, D., 2004, Controls on skarn mineralization and alteration at the Cadia deposits, New South Wales, Australia: Economic Geology, v. 99, p. 761–788.

Fox, N., Harris, A.C., Cooke, D.R., Collett, D., and Faure, K., 2009, Hydrothermal fluid sources in the development of shallow potassic-sodic alteration at the Cadia East alkalic porphyry Au-Cu deposit, NSW: 10th Biennial Meeting of the Society of Geology Applied to Ore Deposits, Townsville, Australia, August 2009, Proceedings, p. 222–224.

Glen, R.A., 2005, The Tasmanides of eastern Australia: London, Geological Society, Special Publications, v. 246, p. 23–96.

Glen, R.A., Walshe, J.L., Barron, L.M., and Watkins, J.J., 1998, Ordovician convergent-margin volcanism and tectonism in the Lachlan sector of East Gondwana: Geology, v. 26, p. 751–754.

Glen, R.A., Crawford, A.J., and Cooke, D.R., 2007, Tectonic setting of porphyry Cu-Au mineralisation in the Ordovician-Early Silurian Macquarie Arc, eastern Lachlan orogen, New South Wales: Australian Journal of Earth Sciences, v. 54, p. 465–479.

Green, D.G., 1999, The geology and origin of the Big Cadia skarn, NSW, Australia: Unpublished B.Sc. (Honours) thesis, Hobart, University of Tasmania, 154 p.

Groves, D.I., Bierlein, F., Meinert, L.D., and Hitzman, M.W., 2010, Iron oxide copper-gold (IOCG) deposits through Earth history: Implications for origin, lithospheric setting, and distinction from other epigenetic iron oxide deposits: Economic Geology, v. 105, p. 641–654.

Hargreaves, R., and Ayres, L.D., 1979, Morphology of Archean metabasalt flows, Utik Lake, Manitoba: Canadian Journal of Earth Sciences, v. 16, p. 1452–1466.

Harper, B.L., 2000, Hydrothermal alteration at the Ridgeway porphyry gold-copper deposit, N.S.W.: Unpublished B.Sc. (Honours) thesis, Hobart, University of Tasmania, 130 p.

Harris, A.C., Allen, C.M., Bryan, S.E., Campbell, I.H., Holcombe, R.J., and Palin, J.M., 2004, ELA-ICP-MS U-Pb zircon geochronology of regional volcanism hosting the Bajo de la Alumbrera Cu-Au deposit: Implications for porphyry-related mineralization: Mineralium Deposita, v. 39, p. 46–67.

Harris, A.C., Bryan, S.E., and Holcombe, R.J., 2006, Volcanic setting of the Bajo de la Alumbrera porphyry Cu-Au deposit, Farallon Negro Volcanics, northwest Argentina: Economic Geology, v. 101, p. 71–94.

Hirata, T., and Nesbitt, R.W., 1995, U-Pb isotope geochronology of zircon—evaluation of the laser probe-inductively coupled plasma-mass spectrometry technique: Geochimica et Cosmochimica Acta, v. 59, p. 2491–2500.

Holliday, J.R., Wilson, A.J., Blevin, P.L., Tedder, I.J., Dunham, P.D., and Pfitzner, M., 2002, Porphyry gold-copper mineralisation in the Cadia district, eastern Lachlan fold belt, New South Wales, and its relationship to shoshonitic magmatism: Mineralium Deposita, v. 37, p. 100–116.

Horn, I., Rudnick, R.L., and McDonough, W.F., 2000, Precise elemental and isotope ratio determination by simulation solution nebulisation and laser ablation-ICP-MS: Application to U-Pb geochronology: Chemical Geology, v. 164, p. 281–301.

Kano, K., 1991, Miocene pillowed sills in the Shimane Peninsula, SW Japan: Journal of Volcanology and Geothermal Research, v. 48, p. 359–366.

Kitto, J.C., 2005, Lithostratigraphy, alteration, and geochemistry at the Cadia East Au-Cu porphyry deposit, NSW: Unpublished B.Sc. (Honours) thesis, Hobart, University of Tasmania, 136 p.

Meffre, S., Scott, R.J., Glen, R.A., and Squire, R.J., 2007, Re-evaluation of contact relationships between Ordovician volcanic belts and the quartz-rich turbidites of the Lachlan orogen: Geological evolution and metallogenesis of the Ordovician Macquarie Arc, Lachlan orogen, New South Wales: Australian Journal of Earth Sciences, v. 54, p. 363–383.

Mulder, T., and Alexander, J., 2002, The physical character of subaqueous sedimentary density flows and their deposits: Sedimentology, v. 48, p. 269–299.

Packham, G., Percival, I., and Bischoff, G., 1999, Age constraints on strata enclosing the Cadia and Junction Reefs ore deposits of central New South Wales, and tectonic implications: Quarterly Notes—Geological Survey of New South Wales, v. 110, p. 1–12.

Pearce, N.J.G., Perkins, W.T., Westgate, J.A., Gorton, M.P., Jackson, S.E., Neal, C.R., and Chenery, S.P., 1997, A compilation of new and published major and trace element data for NIST SRM 610 and NIST SRM 612 glass reference materials: Geostandards, v. 21, p. 115–144.

Percival, I.G., and Glen, R.A., 2007, Ordovician to earliest Silurian history of the Macquarie Arc, Lachlan orogen, New South Wales: Geological evolution and metallogenesis of the Ordovician Macquarie Arc, Lachlan orogen, New South Wales: Australian Journal of Earth Sciences, v. 54, p. 143–165.

Pichler, H., 1965, Acid hyaloclastites: Bulletin Volcanologique, v. 28, p. 293–310.

Pickett, J.W., 1992, Conodont assemblages from limestones north of 'Millamolong', via Mandurama (Palaeontological Report 92/11): Geological Survey of New South Wales Unpublished Report, GS1992/356.

Pogson, D.J., and Watkins, J.J., eds., 1998, Bathurst 1:250 000 Geological Sheet SI/55-8 explanatory notes: Sydney, Geological Survey of New South Wales, 430 p.

Rickards, R.B., and Wright, A.J., 2004, Early Silurian graptolites from Cadia, New South Wales: Proceedings of the Linnean Society of New South Wales, v. 125, p. 173–175.

Rickards, R.B., Percival, I.G., Simpson, A.J., and Wright, A.J., 2001, Silurian biostratigraphy of the Cadia area, south of Orange, New South Wales: Proceedings of the Linnean Society of New South Wales, v. 123, p. 173–191.

Simpson, C.J., Scott, R.J., Crawford, A.J., and Meffre, S., 2007, Volcanology, geochemistry and structure of the Ordovician Cargo Volcanics in the Cargo-Walli region, central New South Wales: Australian Journal of Earth Sciences, v. 54, p. 315–352.

Smith, G.A., 1986, Coarse-grained nonmarine volcaniclastic sediment: Terminology and depositional process: Geological Society of America Bulletin, v. 97, p. 1–10.

Squire, R.J., 2001, Volcanological and tectono-magmatic evolution of the Cadia-Neville region, NSW: Unpublished Ph.D. thesis, Hobart, University of Tasmania, 221 p.

Squire, R.J., and Crawford, A.J., 2007, Magmatic characteristics and geochronology of Ordovician igneous rocks from the Cadia-Neville region, New South Wales; implications for tectonic evolution: Geological evolution and metallogenesis of the Ordovician Macquarie Arc, Lachlan orogen, New South Wales: Australian Journal of Earth Sciences, v. 54, p. 293–314.

Squire, R.J., and McPhie, J., 2002, Characteristics and origin of peperite involving coarse-grained host sediment: Journal of Volcanology and Geothermal Research, v. 114, p. 45–61.

——2007, Complex volcanic facies architecture of the Forest Reefs Volcanics near Cadia, New South Wales, associated with prolonged arc-related volcanism: Australian Journal of Earth Science, v. 54, p. 273–292.

Stevens, N.C., 1957, Further notes on Ordovician formations of central New South Wales: Journal and Proceedings of the Royal Society of New South Wales, v. 90, p. 44–50.

Trotter, J.A., and Webby, B.D., 1995, Upper Ordovician conodonts from the Malongulli Formation, Cliefden Caves area, central New South Wales: Australian Geological Survey Organisation Journal of Australian Geology and Geophysics, v. 15, p. 475–499.

Walker, G.P.L., 1978, Explosive volcanic eruptions: Geologische Rundschau, v. 62, p. 431–446.

Washburn, M., 2008, Architecture of the Silurian sedimentary cover sequence in the Cadia porphyry Au-Cu district, NSW, Australia: Implication for post-mineral deformation: Unpublished M.Sc. thesis, Vancouver, University of British Columbia, 165 p.

Webby, B., Cooper, R., Bergström, S.M., and Paris, F., 2004, Stratigraphic framework and time slices. The great Ordovician biodiversification event: New York, Columbia University Press, p. 41–47.

Wellman, P., and McDougall, I., 1974, Cainozoic igneous activity in eastern Australia: Tectonophysics, v. 23, p. 49–65.

White, J.D.L., 1996, Pre-emergent construction of a lacustrine basaltic volcano, Pahvant Butte, Utah (USA): Bulletin of Volcanology, v. 58, p. 249–262.

White, J.D.L., McPhie, J., and Skilling, I., 2000, Peperite: A useful genetic term: Bulletin of Volcanology, v. 62, p. 65–66.

Wilson, A.J., 2003, The geology, genesis and exploration context of the Cadia gold-copper porphyry deposits, New South Wales, Australia: Unpublished Ph.D. thesis, Hobart, University of Tasmania, 335 p.

Wilson, A.J., Cooke, D.R., and Harper, B.L., 2003, The Ridgeway gold-copper deposit: A high-grade alkalic porphyry deposit in the Lachlan fold belt, New South Wales, Australia: Economic Geology, v. 98, p. 1637–1666.

Wilson, A.J., Cooke, D.R., Stein, H.J., Fanning, C.M., Holliday, J.R., and Tedder, I.J., 2007a, U-Pb and Re-Os geochronologic evidence for two alkalic porphyry ore-forming events in the Cadia district, New South Wales, Australia: Economic Geology, v. 102, p. 3–26.

Wilson, A.J., Cooke, D.R., Harper, B.J., and Deyell, C.L., 2007b, Sulfur isotopic zonation in the Cadia district, southeastern Australia; exploration significance and implications for the genesis of alkalic porphyry gold-copper deposits: Tectonics to mineral discovery; deconstructing the Lachlan orogen: Mineralium Deposita, v. 42, p. 465–487.

Zhen, Y.Y., and Percival, I.G., 2004, Darriwilian (Middle Ordovician) conodonts from the Weemalla Formation, south of Orange, New South Wales: Memoirs of the Association of Australasian Palaeontologists, v. 30, p. 153–178.

Zhen, Y.Y., Webby, B.D., and Barnes, C.R., 1999, Upper Ordovician conodonts from the Bowan Park succession, central New South Wales, Australia: Geobios, v. 32 , p. 73–104.